Research Article
Liver transplantation

JOURNAL
OF HEPATOLOGY

Boosting compromised SARS-CoV-2-specific immunity with mRNA vaccination in liver transplant recipients

Hendrik Luxenburger[1,2,†], **David B. Reeg**[1,†], **Julia Lang-Meli**[1,2,†], Matthias Reinscheid[1,3], Miriam Eisner[4,5], Dominik Bettinger[1], Valerie Oberhardt[1], Elahe Salimi Alizei[1], Katharina Wild[1], Anne Graeser[1], Vivien Karl[1,3], Sagar[1], Florian Emmerich[6], Florian Klein[7,8,9], Marcus Panning[10], Daniela Huzly[10], Bertram Bengsch[1,11], Tobias Boettler[1], Roland Elling[4,5], Robert Thimme[1,*,#], Maike Hofmann[1,*,#], Christoph Neumann-Haefelin[1,*,#]

Journal of Hepatology **2023**. vol. ■ | 1–11

Background & Aims: Liver transplant recipients (LTRs) demonstrate a reduced response to COVID-19 mRNA vaccination; however, a detailed understanding of the interplay between humoral and cellular immunity, especially after a third (and fourth) vaccine dose, is lacking.
Methods: We longitudinally compared the humoral, as well as CD4+ and CD8+ T-cell, responses between LTRs (n = 24) and healthy controls (n = 19) after three (LTRs: n = 9 to 16; healthy controls: n = 9 to 14 per experiment) to four (LTRs: n = 4; healthy controls: n = 4) vaccine doses, including in-depth phenotypical and functional characterization.
Results: Compared to healthy controls, development of high antibody titers required a third vaccine dose in most LTRs, while spike-specific CD8+ T cells with robust recall capacity plateaued after the second vaccine dose, albeit with a reduced frequency and epitope repertoire compared to healthy controls. This overall attenuated vaccine response was linked to a reduced frequency of spike-reactive follicular T helper cells in LTRs.
Conclusion: Three doses of a COVID-19 mRNA vaccine induce an overall robust humoral and cellular memory response in most LTRs. Decisions regarding additional booster doses may thus be based on individual vaccine responses as well as evolution of novel variants of concern.

Introduction

Due to immunosuppression and comorbidities, liver transplant recipients (LTRs) represent a vulnerable group with significantly increased risk of developing symptomatic SARS-CoV-2 infection compared to the general population.[1,2] Accordingly, the European Association for the Study of the Liver clearly recommends vaccination for LTRs.[3] However, as seen after natural infection, the seroconversion and T-cell response rates in LTRs after mRNA vaccination are lower than in healthy individuals, who are known to develop robust vaccine-induced antibody and T-cell responses.[4–12] To date, most studies in LTRs assessed the virus-specific cellular and humoral immune response after two mRNA vaccine doses. Recent data suggest that antibody and T-cell responses are enhanced by a third and fourth vaccine dose.[13–15] However, although essential for evaluating future vaccination strategies, a detailed understanding of T-cell phenotype, memory formation and the interplay of different cellular and humoral compartments of the immune response after SARS-CoV-2 vaccination in LTRs is still lacking. For example, reduced antibody levels might be explained by a different subset distribution of CD4+ T cells, since strong antibody responses are associated with higher levels of follicular T helper (T_{FH}) cells in immunocompetent individuals.[16] Therefore, we aimed to investigate the impact of repeated booster vaccinations on the effector arm of the adaptive immune response focusing on SARS-CoV-2-specific CD8+ T cells and the coordinating function of the CD4+ T-cell response. Overall, we performed the first, to our knowledge, in-depth characterization of CD4+ and CD8+ T cells in LTRs following administration of up to four vaccine doses.

Patients and methods

Study cohort

Twenty-four LTRs and 19 healthy controls (HCs) without liver pathology who received up to four doses of an mRNA vaccine

Keywords: COVID-19; vaccine response; liver transplantation; immunosuppression; immunological memory.
Received 25 October 2022; received in revised form 10 January 2023; accepted 4 February 2023; available online xxx
* Corresponding authors Address: Department of Medicine II, Freiburg University Medical Center, Hugstetter Straße 55, 79106 Freiburg, Germany. (R. Thimme), or . (M. Hofmann), or . (C. Neumann-Haefelin).
E-mail addresses: robert.thimme@uniklinik-freiburg.de (R. Thimme), maike.hofmann@uniklinik-freiburg.de (M. Hofmann), christoph.neumann-haefelin@uniklinik-freiburg.de (C. Neumann-Haefelin).
† Equal contribution
# Shared last authors
https://doi.org/10.1016/j.jhep.2023.02.007

(BNT162b2/Comirnaty or mRNA-1273/Spikevax) were recruited at the Freiburg University Medical Center, Germany. HLA-typing was performed by next-generation sequencing. Donor characteristics are summarized in Table S1.

Ethics

Written informed consent was obtained from all participants before inclusion. The study was conducted according to federal guidelines and local ethics committee regulations (Albert-Ludwigs-Universität, Freiburg, Germany; vote: 322/20, 21-1135 and 315/20) and the Declaration of Helsinki (1975).

PBMC isolation

Peripheral blood mononuclear cell (PBMC) isolation is described in the supplementary information.

In vitro expansion and intracellular IFNγ staining with overlapping peptides

We tested a total of 182 overlapping peptides (OLPs) spanning the entire SARS-CoV-2 spike protein sequence (Gene Bank Accession code MN908947.3), synthesized as 18-mers overlapping by 11 amino acids with a free amine NH_2 terminus and a free acid COOH terminus with standard Fmoc chemistry showing a purity of >70% (Genaxxon Bioscience). Details regarding the experimental procedure are provided in the supplementary information.

Peptides and tetramers for T-cell analysis

The peptides for A*02/S_{269} (YLQPRTFLL) and A*03/S_{378} (KCYGVSPTK) were synthesized with an unmodified N terminus and an amidated C terminus with standard Fmoc chemistry and a purity of >70% (Genaxxon Bioscience). Peptides were then loaded on HLA class I easYmers (immunAware) according to the manufacturer's instructions. For tetramerization, the SARS-CoV-2 peptide-loaded HLA class I monomers were subsequently incubated together with phycoerythrin- or allophycocyanin-conjugated streptavidin (Agilent) following the manufacturer's protocol.

In vitro expansion of spike-specific CD8+ T cells and assessment of effector function

After stimulation of approximately 1.5×10^6 PBMCs with A*02/S269 (YLQPRTFLL) or A*03/S378 (KCYGVSPTK) peptides (5 μM) and an anti-CD28 monoclonal antibody (0.5 μg ml^{-1}, BD), the cells were expanded for 14 days in complete RPMI culture medium containing recombinant IL-2 (20 IU ml^{-1}, StemCell Technologies). Intracellular cytokine production and degranulation was assessed with spike-derived peptides (15 μM) in the presence of anti-CD107a (H4A3, 1:100, BD Bioscience) for 1 h at 37 °C. Brefeldin A (GolgiPlug, 0.5 μl ml^{-1}) and monensin (GolgiStop, 0.5 μl ml^{-1}) (both BD Biosciences) were then added for an additional 4 h, followed by surface and intracellular staining. Calculation of the expansion capacity was based on peptide-loaded HLA class I tetramer staining as previously described.[17]

Magnetic bead-based enrichment of spike-specific CD8+ T cells

Enrichment of spike-specific CD8+ T cells is described in the supplementary information.

Multiparametric flow cytometry for T-cell analysis

A list of the antibodies used for multiparametric flow cytometry is provided in the supplementary CTAT table. To conduct the staining for intranuclear and cytoplasmic molecules, respectively, FoxP3/Transcription Factor Staining Buffer Set (Thermo Fisher) and Fixation/Permeabilization Solution Kit (BD Biosciences) were used according to the manufacturer's protocol. Analyses were performed on FACSCanto II with FACSDiva software version 10.6.2 (BD) or CytoFLEX (Beckman Coulter) with CytExpert Software version 2.3.0.84 after fixation of cells in 2% paraformaldehyde (Sigma). Data were then analyzed with FlowJo 10.7.1 (Treestar). The gating strategy is displayed in Fig. S1 and S2.

Dimensionality reduction of multiparametric flow cytometry data

Dimensionality reduction of flow cytometry data was performed with R version 4.1.3 using the Bioconductor CATALYST package (version 1.18.1). Tetramer-positive CD8+ T cells were defined with the help of FlowJo 10. Only samples with ≥5 spike-specific CD8+ T cells were included in the dimensionality reduction analysis. To compensate for the lower abundance of this population in LTRs, cell counts were sampled down to a maximum of 35 cells per patient and time point. In addition, marker expression intensities were transformed, applying arcsinh-transformation with a cofactor of 150 in order to facilitate visualization. The R code for reproduction of the described analyses is accessible at https://github.com/sagar161286/SARSCoV2_specific_CD8_Tcells.

Activation-induced marker (AIM) assay

Briefly, three wells containing 3×10^5 PBMCs each were prepared per patient and time point using a sterile 96-well U-bottom plate. Cells were incubated with DMSO (50 mg ml^{-1}; negative control), spike-OLP-pool (10 μg ml^{-1}) or phytohemagglutinin (10 μg ml^{-1}; positive control) for 1 h at 37 °C. After a washing step, 1.2×10^6 PBMCs were added (total cell number per well about 1.5×10^6 cells) and stimulated again with lower concentrations of the three reagents (DMSO 5 mg ml^{-1}, spike-OLP-pool 1 μg ml^{-1} and phytohemagglutinin 5 μg ml^{-1}) for 24 h at 37 °C. Chemokine receptor antibodies (CCR6, CCR7, CXCR and CXCR5) were added during both stimulations in their respective concentrations stated in the supplementary CTAT table. Thereafter, multiparametric flow cytometry was performed. Spike-specific CD4+ T cells were determined via the co-expression of OX40 and CD137 after the stimulation process. The CD4+ T-cell subsets were defined by CXCR5, CXCR3 and CCR6. The gating strategy is displayed in Fig. S3.

Serum IgG determination

SARS-CoV-2-specific antibodies were determined by anti-SARS-CoV-2-QuantiVac-ELISA (IgG) from Euroimmun. Detection of anti-SARS-CoV-2 spike-specific IgGs was performed

according to the manufacturer's instructions (anti-SARS-CoV-2 S-IgG; <35.2 BAU ml^{-1}: negative, ≥35.2 BAU ml^{-1}: positive).

SARS-CoV-2 pseudovirus neutralization assay

Pseudovirus neutralization assays against SARS-CoV-2 wild-type (Wuhan-Hu-1) and the Omicron BA.4/BA.5 variants were performed on a selection of 47 samples as described in the supplementary information.

Statistical analysis

Statistical analysis was performed with Prism 9 (GraphPad Software) and STATA version 15.0 (StataCorp Lp, Texas). Two-tailed Mann-Whitney *U* tests, two-sided Wilcoxon matched-pairs signed rank tests, Kruskal-Wallis tests, two-way ANOVAs with full model and spearman correlations were used to assess statistical significance. A p value <0.05 was considered statistically significant.

Results

Impaired adaptive effector response in LTRs *vs.* HCs after three doses of mRNA vaccination

We obtained time point-matched samples during the course of vaccination in LTRs (total, n = 24) and age-matched HCs (total, n = 19) after up to four SARS-CoV-2 vaccine doses (Fig. S4A,B). All individuals received mRNA vaccinations (BNT162b2/Comirnaty or mRNA-1273/Spikevax) and did not have a history of SARS-CoV-2 infection (all tested negative for N-IgG) (Table S1). All LTRs received calcineurin inhibitors and most patients additionally received mycophenolate mofetil (MMF) as an immunosuppressive treatment (Fig. S4C).

LTRs (n = 16) showed significantly lower levels of spike-specific IgG after three mRNA vaccine doses compared to HCs (n = 14) (Fig. 1A). We also analyzed spike-specific CD8+ T-cell responses after the third vaccination in LTRs (n = 9) and HCs (n = 9) using OLPs spanning the whole spike protein. LTRs

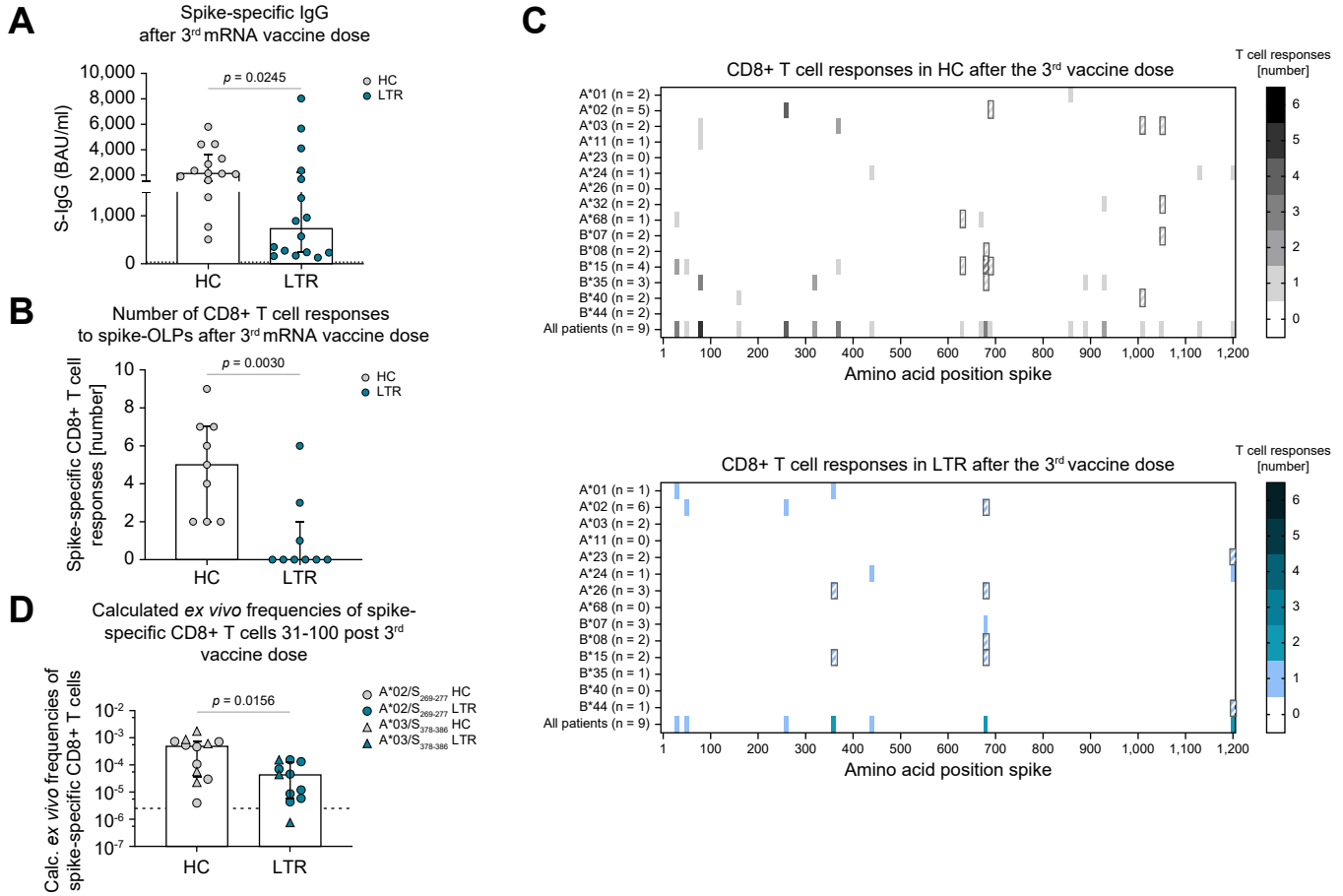

Fig. 1. Impaired adaptive effector response in LTRs *vs.* HCs after three doses of mRNA vaccination. (A) Spike-specific IgG-levels in HCs and LTRs after the 3rd vaccine dose (LTRs n = 16, HCs n = 14). (B) Numbers of CD8+ T-cell responses to spike-OLPs after *in vitro* expansion per patient after the 3rd vaccine dose (HCs n = 9; LTRs n = 9). (C) Number and location of CD8+ T-cell responses to spike-OLPs after *in vitro* expansion in HCs (top) *vs.* LTRs (bottom) after the 3rd vaccine dose. Numbers of tested individuals (per HLA allotype and in total) are indicated. OLPs with >1 HLA-matched previously described epitopes are crosshatched. (D) *Ex vivo* frequency of spike-specific CD8+ T cells in HCs and LTRs after the 3rd vaccine dose (HCs n = 12; LTRs n = 11). Cut-off for positive responses is indicated by a dashed line. Statistics: Mann-Whitney *U* test (A, B, D). HCs, healthy controls; LTRs, liver transplant recipients; OLPs, overlapping peptides.

showed significantly lower numbers of spike-specific CD8+ T-cell responses (Fig. 1B). For all positive responses, we identified the previously described optimal epitope restricted by an HLA class I allele expressed by the respective individual. If no HLA-matched epitope was previously described, we conducted an *in silico* prediction to determine the most likely amino acid sequence and HLA class I restriction of the optimal epitope. Using this comprehensive approach, we found a reduced breadth of spike-specific CD8+ T-cell responses in the cohort of LTRs compared to HCs (Fig. 1C). Of note, the herein detected CD8+ T-cell epitopes for LTRs and HCs are largely conserved in SARS-CoV-2 variants of concern (VOC), for instance BA.1, BA.4/5 or BQ.1 (Fig. S5A,B).

Complementing the comprehensive analysis of the CD8+ T-cell repertoire, we performed *ex vivo* peptide/MHC I tetramer-based enrichment of spike-specific CD8+ T cells targeting two immunodominant epitopes (A*02/$S_{269-277}$ and A*03/$S_{378-386}$) in time point-matched samples 31-100 days after a third SARS-CoV-2 mRNA vaccination in HCs (n = 12) and LTRs (n = 11). This method is limited to selected epitopes; however, it is also very sensitive in detecting vaccine-induced CD8+ T-cell responses.[18] On the single-epitope level, LTRs showed significantly reduced frequencies of spike-specific CD8+ T cells compared to HCs (Fig. 1D). Of note, reduced frequencies of spike-specific CD8+ T cells in LTRs compared to HCs were already detectable after the second dose of SARS-CoV-2 mRNA vaccination and were accompanied by significantly lower expression levels of CD38 and T-BET (Fig. S6A, B). This observation points towards reduced activation and subsequent effector T-cell differentiation in LTRs compared to HCs.

Overall, our data indicate an impaired humoral and cellular effector immune response characterized by a narrow CD8+ T-cell repertoire and reduced frequencies of spike-specific CD8+ T-cell responses in LTRs *vs.* HCs after administration of three doses of a SARS-CoV-2 mRNA vaccine.

Little effect of mRNA booster vaccination on the cellular effector response in LTRs

To determine the effect of repeated SARS-CoV-2 mRNA vaccine boosters on the effector arm of the adaptive immune system, we analyzed spike-specific IgG, the CD8+ T-cell repertoire using OLPs and *ex vivo* frequencies of spike-specific CD8+ T-cell responses applying peptide/MHC I tetramer-based enrichment longitudinally at different time points after the second, third and fourth vaccine dose. Overall, we found significantly lower levels of spike-specific IgG in LTRs *vs.* HCs, but a significant booster effect of repeated mRNA vaccine boosters that was more prominent in LTRs compared to HCs (Fig. 2A). In contrast to the humoral immune response, the number of spike-specific CD8+ T-cell responses remained similar in LTRs and HCs tested longitudinally after two (HCs n = 9, LTRs n = 8), three (HCs n = 9, LTRs n = 8) or four (HCs n = 2, LTRs n = 3) vaccine doses using OLPs (Fig. 2B). In line with this observation, the repertoire of spike-specific CD8+ T-cell responses showed a similar pattern in the three patients analyzed longitudinally (Fig. 2C), indicating that repeated vaccine boosters do not substantially induce *de novo* spike-specific CD8+ T-cell responses.

On the single-epitope level, *ex vivo* frequencies of spike-specific CD8+ T-cell responses against the immunodominant A*02/$S_{269-277}$ and A*03/$S_{378-386}$ epitopes were overall significantly lower in LTRs compared to HCs but did not significantly change after a third or fourth vaccine dose for either group (Fig. 2D). Of note, in one LTR, a spike-specific CD8+ T-cell response was only detectable after the fourth mRNA vaccine dose (Fig. S7A), indicating that a subset of LTRs benefit from a fourth vaccine dose. Taken together, the humoral vaccine response is clearly boosted by a third and fourth vaccine dose in LTRs, while the frequency of spike-specific CD8+ T-cell responses already reaches a plateau after the second vaccine dose in most LTRs.

Robust immune memory formation in LTRs

To investigate the effect of mRNA vaccination on the formation of a spike-specific T-cell memory in LTRs, we then compared the phenotype of spike-specific CD8+ T cells at 31-100 days post third vaccination in LTRs (n = 10) *vs.* HCs (n = 12). t-distributed stochastic neighbor embedding analysis of concatenated phenotypic data including BCL-2, CCR7, CD27, CD38, CD45RA, CD95, CD127, T-BET and TCF1 revealed a strong overlap of spike-specific CD8+ T-cell phenotypes in HCs and LTRs; however, with differences regarding expression of T-BET or CD127 (Fig. 3A and Fig. S7B). In line, the memory T-cell subset distribution of spike-specific CD8+ T cells was slightly different in the two cohorts. LTRs showed significantly higher percentages of central memory T cells (defined as CD45RA-CCR7+CD27+) while HCs displayed significantly higher percentages of effector memory cells (defined as CD45RA-CCR7-CD27+) (Fig. S7C). We next assessed the functional *in vitro* capacity of spike-specific CD8+ T cells in LTRs *vs.* HCs. There was no significant difference in expansion capacity, degranulation (represented by CD107a production) or cytokine production (represented by IFNγ production) between spike-specific CD8+ T cells from LTRs and HCs after *in vitro* expansion (Fig. 3B), pointing towards an intact recall capacity of spike-specific CD8+ T cells from LTRs upon optimal stimulation.

To more precisely quantify the spike-specific T-cell memory pool irrespective of certain subsets, we next analyzed CD8+ T cells highly expressing BCL-2 (BCL-2^{hi}). After a third vaccination, there was no difference in absolute calculated frequencies of BCL-2^{hi} spike-specific CD8+ T cells in HCs *vs.* LTRs (Fig. 3C), despite lower overall frequencies of spike-specific CD8+ T cells in LTRs (Fig. 1D). The numbers and the activation/differentiation marker-footprint of BCL-2^{hi} spike-specific CD8+ T cells in LTRs were similar after two, three or four mRNA vaccinations (Fig. 3C,D). However, the phenotype showed minor differences between HCs and LTRs, with a trend towards higher expression of TCF-1 and CD127 in LTRs, while the expression of T-BET was higher in HCs (Fig. 3D and Fig. S7D, upper panels).

Next, we focused on the subset of T memory stem cells (T-SCMs) which are important for long-term immunity. Despite overall lower frequencies of spike-specific CD8+ T cells in LTRs, frequencies of T-SCMs were similar in HCs and LTRs. They remained constant after two, three or four mRNA vaccinations (Fig. 3E). The phenotype of T-SCMs was similar in the two cohorts and also with respect to the longitudinal sampling after two, three or four mRNA vaccine doses (Fig. 3F and Fig. S7D, lower panels).

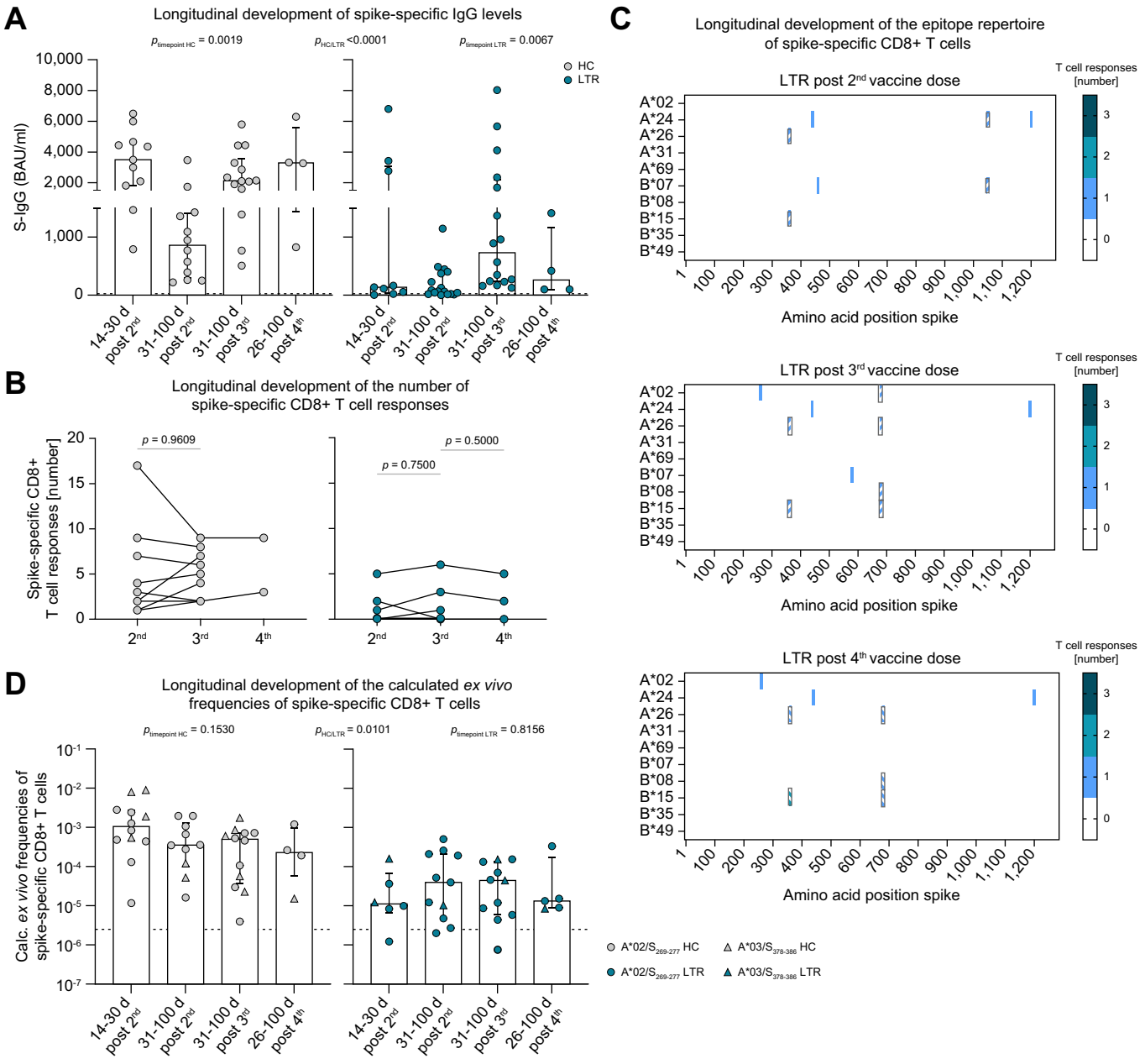

Fig. 2. Small effect of mRNA booster vaccination on the cellular effector response. (A) Spike-specific IgG-levels in HCs and LTRs at 14-30 days after the 2nd (HCs n = 11, LTRs n = 9), 31-100 days after the 2nd (HCs n = 12, LTRs n = 17), 31-100 days after the 3rd (HCs n = 14, LTRs n = 16) or 26-100 days after the 4th (HCs n = 4, LTRs n = 4) vaccination. (B) Number of CD8+ T-cell responses per individual to spike-OLP after *in vitro* expansion in HCs and LTRs followed longitudinally after the 2nd (HCs n = 9, LTRs n = 8), 3rd (HCs n = 9, LTRs n = 8) and 4th (HCs n = 2, LTRs n = 3) vaccine dose. (C) Number and location of CD8+ T-cell responses to spike-OLP after *in vitro* expansion in LTRs (n = 3) after the 2nd, 3rd and 4th mRNA vaccination. OLPs with >1 HLA-matched, previously described, epitopes are crosshatched. (D) Calculated *ex vivo* frequencies of spike-specific CD8+ T cells at 14-30 days after the 2nd (HCs n = 12, LTRs n = 6), 31-100 days after the 2nd (HCs n = 10, LTRs n = 11), 31-100 days after the 3rd (HCs n = 12, LTRs n = 11) or 26-100 days after the 4th (HCs n = 4, LTRs n = 5) vaccine dose. Cut-off for positive responses is indicated by a dashed line. Statistics: Wilcoxon matched-pairs signed rank test (B) and two-way ANOVA for multiple comparison (A, D) to examine the effect of condition (HCs *vs.* LTRs), as well as Kruskal-Wallis test (A, D) to examine the effect of vaccination time point on spike-specific IgG levels and CD8+ T-cell frequencies. HCs, healthy controls; LTRs, liver transplant recipients; OLPs, overlapping peptides.

Taken together, the formation of a functional spike-specific CD8+ T-cell memory pool seems to be intact in LTRs, despite the overall reduced numbers and frequencies of spike-specific CD8+ T cells. The spike-specific memory pool in LTRs is constant over time without a clear booster or compromising effect of the third or fourth vaccine dose.

Similar breadth and frequencies of spike-specific CD4+ T cells in HCs and LTRs after mRNA vaccination

Next, to assess the coordinating helper arm of the adaptive immune response in LTRs after mRNA vaccination, we used OLPs to map spike-specific CD4+ T-cell responses after two and three doses of SARS-CoV-2 mRNA vaccination. HCs and

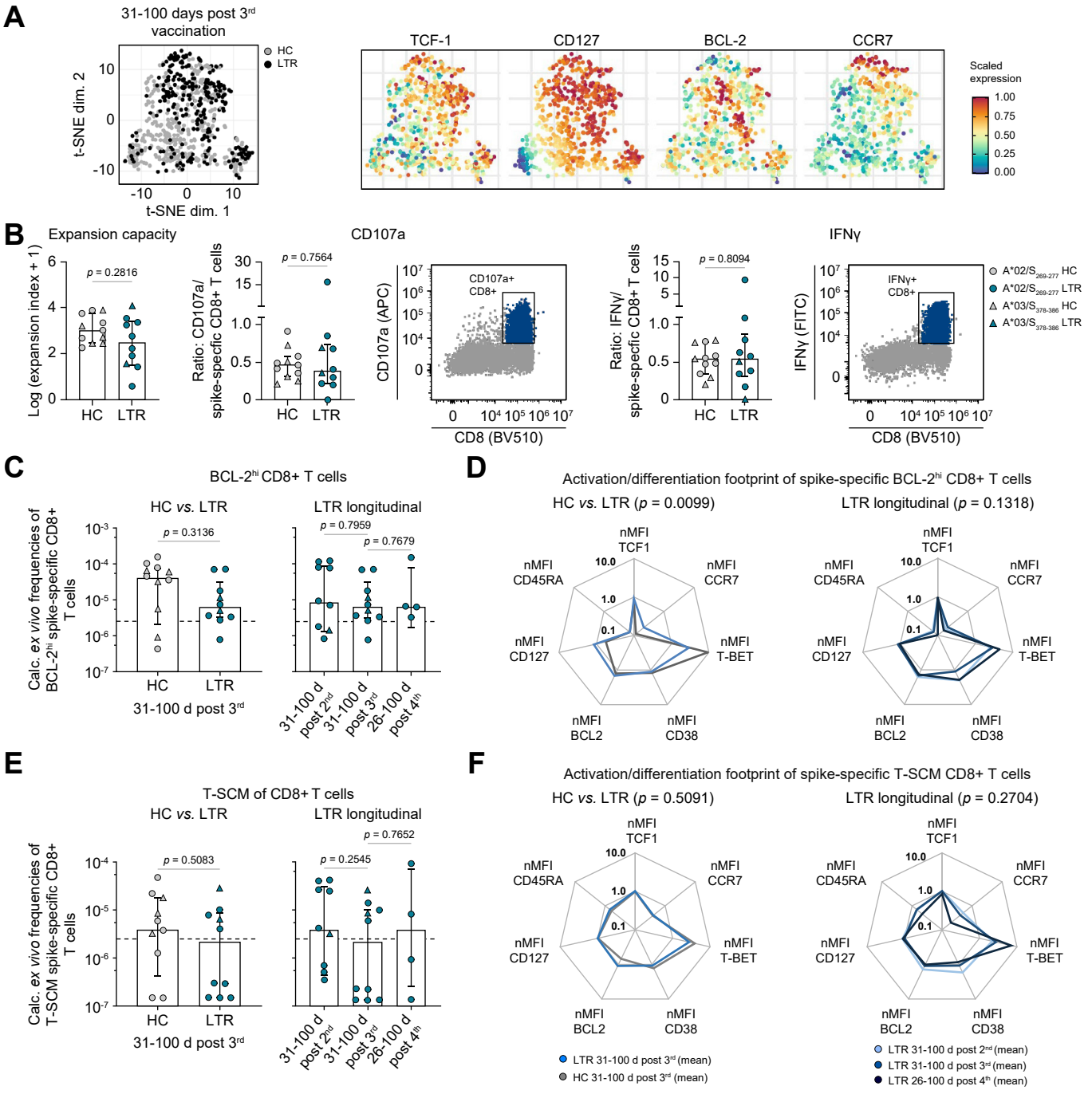

Fig. 3. Maintenance of the adaptive effector response in LTRs. (A) t-SNE representation of *ex vivo* flow cytometry data comparing spike-specific CD8+ T cells derived from HCs and LTRs at 31-100 days after the 3rd vaccine dose (expression levels of TCF-1, CD127, BCL-2 and CCR7). (B) Functional capacities of spike-specific CD8+ T cells after *in vitro* expansion (31-100 days post 3rd vaccine dose; LTRs n = 10; HCs n = 11). (C–F) Calculated *ex vivo* frequencies of spike-specific CD8+ T cells with high BCL-2 expression (BCL-2hi) (C) or of the spike-specific CD8+ T-SCM subset (CD45RA+CCR7+CD27+CD95+) (E) in LTRs *vs.* HCs. nMFI of different markers within the subset of BCL-2hi (D) or T-SCM (F) spike-specific CD8+ T cells in HCs and LTRs normalized to naïve CD8+ T cells; samples with ≥5 cells per subset are depicted. Statistics: Mann-Whitney *U* test (B, C, E), two-way ANOVA for multiple comparison (D, F) to examine the effect of condition (HCs *vs.* LTRs; left) or time point (right) on memory subsets. HCs, healthy controls; LTRs, liver transplant recipients; nMFI, mean fluorescence intensity; T-SCM, T memory stem cell; t-SNE, t-distributed stochastic neighbor embedding.

LTRs showed similar numbers of spike-specific CD4+ T-cell responses after a third vaccine dose (Fig. 4A). In addition, the breadth of the spike-specific CD4+ T-cell repertoire was similar in LTRs and HCs after three vaccine doses (Fig. 4B). In LTRs followed longitudinally after the second (n = 8), third (n = 8) and fourth (n = 3) vaccine dose, we did not observe a significant increase in spike-specific CD4+ T-cell responses per patient with repeated vaccinations, although some variation in the number of responses was apparent (Fig. 4C). The pattern of the targeted epitopes of spike-specific CD4+ T-cell responses in

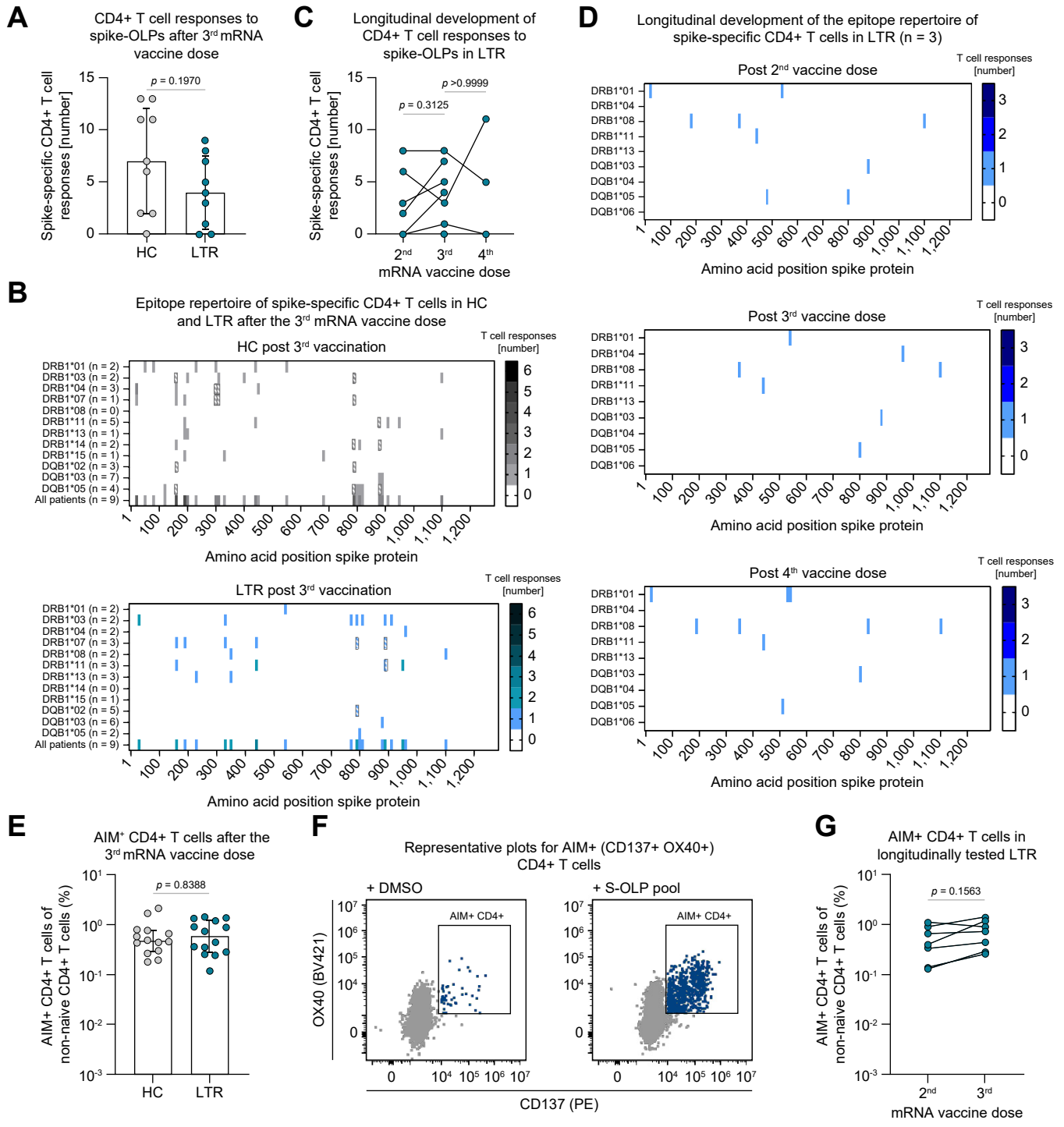

Fig. 4. Similar breadth of the spike-specific CD4+ T-cell epitope repertoire in LTRs and HCs after mRNA vaccination. (A) Numbers of CD4+ T-cell responses to spike-OLP after *in vitro* expansion per individual after the 3rd (HCs n = 9; LTRs n = 9) vaccine dose. (B) Number and location of spike-specific CD4+ T-cell responses to spike-OLP after *in vitro* expansion in HCs *vs.* LTRs after the 3rd vaccine dose, numbers of tested individuals (per HLA allotype and in total) are indicated. OLP with > 1 HLA-matched previously described epitopes are crosshatched. (C) Numbers of CD4+ T-cell responses to spike-OLP after *in vitro* expansion per individual tested longitudinally in LTRs after the 2nd (n = 8), 3rd (n = 8) and 4th (n = 3) mRNA vaccine dose. (D) Number and location of CD4+ T-cell responses to spike-OLP after *in vitro* expansion in LTRs (n = 3) tested longitudinally after the 2nd, 3rd and 4th mRNA vaccine dose. (E-G) *Ex vivo* frequencies of AIM+ (CD137+ OX40+) CD4+ T cells after the 3rd mRNA vaccine dose (E, HCs n = 14, LTRs n = 14) with representative plots (F) and tested longitudinally after the 2nd (n = 7) and 3rd (n = 7) mRNA vaccine dose (G). Statistics: Mann-Whitney *U* test (A, E) and Wilcoxon matched-pairs signed rank test (C, G). HCs, healthy controls; LTRs, liver transplant recipients; OLP, overlapping peptide.

the three LTRs followed longitudinally up to a fourth vaccination was similar after two, three and four vaccine doses (Fig. 4D), indicating that few spike-specific CD4+ T-cell responses were induced *de novo* after repeated vaccine boosters. Importantly, up to 30% of the herein defined CD4+ T-cell epitopes for LTRs and HCs are affected by amino acid substitutions in SARS-CoV-2 VOC such as BA.1, BA.4/5 or BQ.1 (Fig. S8A,B). To gain further insights into the characteristics of vaccine-induced

spike-specific CD4+ T cells in LTRs, we subsequently stimulated PBMCs using the spike-OLP-pool and analyzed the co-expression of the activation-induced markers (AIM) CD137 and OX40. In line with the results described above, LTRs showed similar frequencies of AIM+ CD4+ T cells after the third vaccine dose compared to HCs (Fig. 4E,F). Furthermore, in patients studied longitudinally, there was no significant increase in the frequency of activated CD4+ T cells following the third vaccine dose compared to the second dose (Fig. 4G). Our data indicate that, in contrast to the spike-specific humoral and CD8+ T-cell-mediated immune response, the overall spike-specific CD4+ T-cell response in LTRs resembles its counterpart in HCs after three SARS-CoV-2 mRNA vaccine doses, with respect to frequencies and breadth.

Altered subset distribution of spike-specific CD4+ T cells in LTRs after mRNA vaccination is associated with impaired adaptive effector responses

To investigate the effect of liver transplantation and subsequent immunosuppressive medication on vaccine-induced CD4+ T-cell polarization, we analyzed the distribution of several CD4+ T-cell subsets within the population of spike-reactive CD4+ T cells (gating strategy is depicted in Fig. S3). Spike-reactive CD4+ T cells were defined as CD137+OX40+ (AIM+) CD4+ T cells after stimulation with the spike-OLP pool.

We observed reduced frequencies of spike-reactive T_{FH} cells in LTRs after the second mRNA vaccine dose (Fig. 5A,B). Importantly, the administration of a third shot resulted in a clear

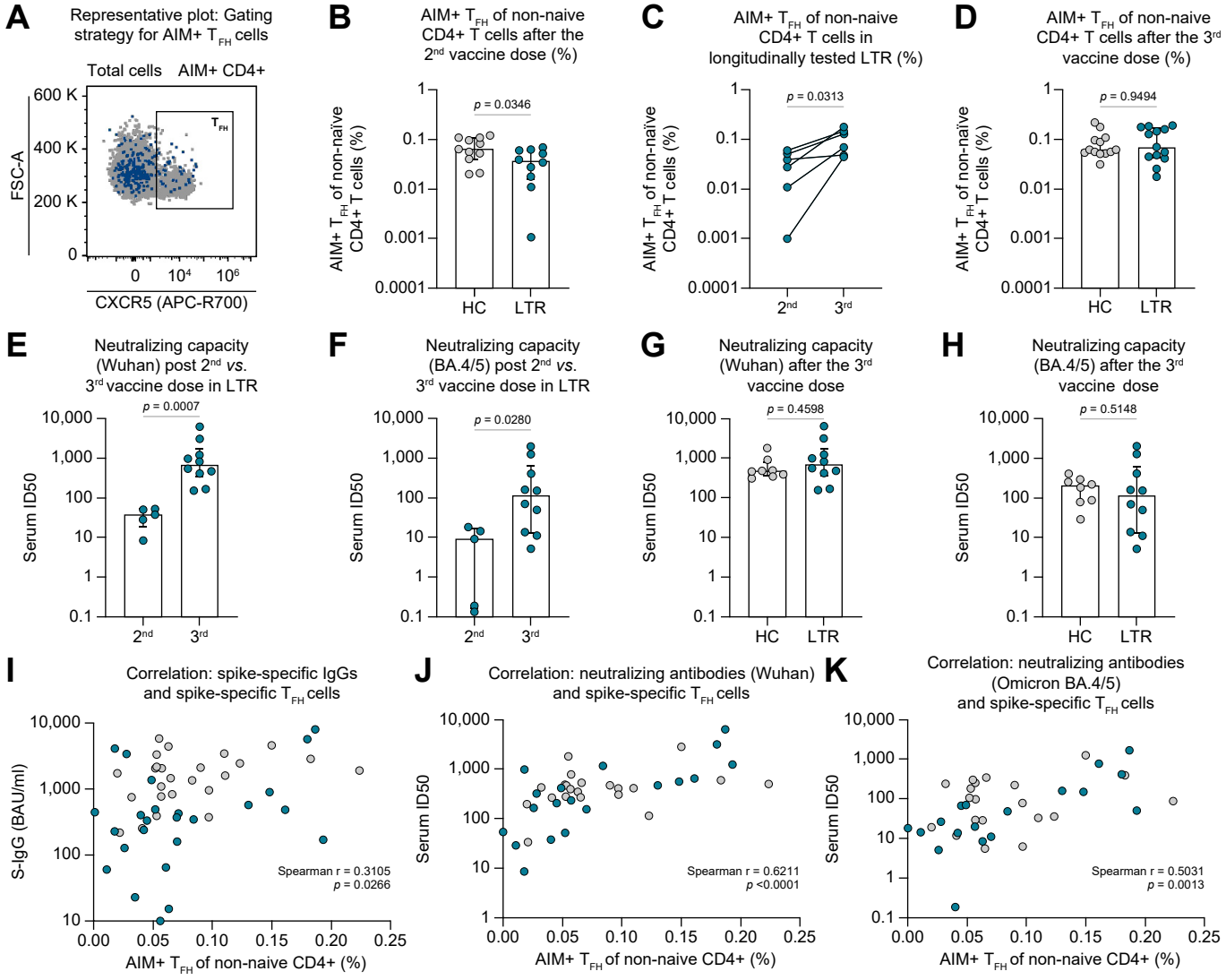

Fig. 5. Altered subset distribution of spike-specific CD4+ T cells in LTRs after mRNA vaccination is associated with impaired adaptive effector response. (A-D) *Ex vivo* proportion of AIM+ (CD137+ OX40+) T_{FH} cells of non-naïve CD4+ T cells (representative dot plot displayed in A) after the 2nd vaccine dose in HCs (n = 11) and LTRs (n = 10) (B), in longitudinally tested LTRs (n = 6) (C) and after the 3rd vaccine dose in HCs (n = 13) and LTRs (n = 13) (D). (E-H) Neutralizing capacity against the SARS-CoV-2 Wuhan strain (E, G) or Omicron BA.4/5 variant (F, H) in LTR samples tested after 2nd (n = 5) and 3rd (n = 10) vaccine dose and in HCs (n = 8) and LTRs (n = 10) after the 3rd vaccine dose. (I) Correlation between the level of spike-specific IgG and the frequencies of spike-specific T_{FH} cells; (J, K) Correlation between the neutralizing capacity against Wuhan (J) or Omicron BA.4/5 (K) variants and the frequencies of spike-specific T_{FH} cells; LTRs and HCs as well as all available vaccination time points were pooled for the correlation analysis. Statistics: Mann-Whitney *U* test (B, D-H), Wilcoxon matched-pairs signed rank test (C) and Spearman correlation (I–K). AIM, activation-induced marker; HCs, healthy control; LTRs, liver transplant recipients; T_{FH}, follicular T helper.

increase in the abundance of this population in longitudinally analyzed LTRs (Fig. 5C,D). In contrast, only minor differences were detectable with regard to other CD4+ T-cell subsets, namely T helper (T_H)1 (CXCR5-CXCR3+CCR6-), T_H17 (CXCR5-CXCR3-CCR6+) and T_H1-like T_H17 (CXCR5-CXCR3+CCR6+) cells, also considering the effect of booster vaccination (Fig. S9A-I). Given the coordinative role of T_{FH} cells within the adaptive immune system, we next wondered whether their initial reduction in LTRs could be linked to the attenuated vaccine-induced humoral response (Fig. 1A, Fig. 2A). To address this question, we also assessed the neutralizing capacity of serum antibodies directed against the SARS-CoV-2 Wuhan and Omicron BA.4/5 variants in selected patients and controls. Of note, the data obtained from the pseudovirus neutralization assays for both variants strongly correlate with the levels of spike-specific IgG (Fig. S10A,B). We noticed an impaired neutralization capacity in LTRs compared to HCs following the second vaccine dose (Fig. S10C,D). However, as for the T_{FH} cell frequencies, a significant increase in the median serum ID50 became evident for both viral variants following the third vaccine shot in LTRs (Fig. 5E,F). In line, the neutralization capacity after the third vaccine dose was similar in LTRs and HCs (Fig. 5G, H). Nonetheless, it is important to note that we still detected a significantly reduced median serum ID50 for the Omicron BA.4/5 variants compared to the Wuhan strain in both LTRs and HCs (Fig. S10E).

Finally, when linking these results to the altered CD4+ T-cell subset distribution in LTRs, positive correlations between the frequency of spike-specific T_{FH} cells and the levels of spike-specific IgG as well as the neutralization capacities against the Wuhan and the Omicron BA.4/5 variants became evident (Fig. 5I-K). Therefore, our data collectively indicate that an imbalanced subset distribution among spike-reactive CD4+ T cells might contribute to the impaired humoral immune response after SARS-CoV-2 mRNA vaccination in LTRs.

Discussion

Our findings suggest that i) the long-term humoral and cellular effector response up to 100 days post vaccination is numerically impaired in LTRs compared to HCs, while the induced CD8+ T-cell memory phenotype is comparable in the two cohorts; ii) an imbalanced subset distribution among spike-reactive CD4+ T cells might contribute to the impaired effector immune response after SARS-CoV-2 mRNA vaccination in LTRs; and iii) there is only a limited long-term booster effect induced by a third or fourth vaccination especially on the CD8+ T-cell response in LTRs, at least in the majority of patients.

To our knowledge, this study is the first to comprehensively analyze the landscape of vaccine-induced humoral and CD4+ and CD8+ T-cell responses after up to four SARS-CoV-2 mRNA vaccine doses in LTRs. Our aim was to identify immunological mechanisms that contribute to the impaired vaccine-induced immune response. Of note, our work was not powered to identify general risk factors for reduced humoral or cellular vaccine responses among LTRs, which have already been described.[9,11,13,14] Established clinical characteristics associated with reduced antibody levels or overall spike-specific T-cell responses are higher age, combined immunosuppressive treatment and treatment with MMF >1 g/day.[9] Importantly, donors with these risk factors were prevalent in our cohort, with the majority (18/24) of patients receiving combined immunosuppression, 64% receiving MMF and 24% receiving MMF doses >1 g/d.

In line with previous reports, we detected a lower humoral[9] and cellular[11] immunogenicity of the SARS-CoV-2 mRNA vaccination in the vulnerable group of LTRs compared to HCs. Our phenotypical analysis of the spike-specific CD8+ T-cell response adds the important finding that an intact stem cell memory population of spike-specific CD8+ T cells, similar to HCs, is already induced after two mRNA vaccine doses in most LTRs despite the numerical impairment. This memory population is especially relevant for long-term immunity and thus maintenance of T-cell memory.[10]

With regard to vaccine-induced CD4+ T cells, the importance of virus-specific CD4+ T-cell help for the coordination of the adaptive immune response is well established.[19] In addition to T_H1 cells, a subset of particular interest in this regard are T_{FH} cells. Notably, despite an overall comparable quantity and breadth of spike-specific CD4+ T cells in both cohorts, we observed lower frequencies of T_{FH} cells in LTRs, particularly after the second vaccine dose. While their role in organizing the humoral response has already been emphasized by multiple studies,[20] recent findings also suggest that T_{FH} cells are involved in the maintenance of the effector CD8+ T-cell response.[21,22] In line with these results, we noticed a correlation between the amounts of spike-specific T_{FH} cells and the levels of S-IgG, as well as the neutralization capacity against the SARS-CoV-2 Wuhan and Omicron BA.4/5 variants. Hence, the decreased number of T_{FH} cells in LTRs after two vaccine doses might be linked to the impaired humoral response, similar to observations in kidney transplant recipients.[23] Importantly, however, the application of a third vaccine dose increased the levels of T_{FH} cells, S-IgG and the neutralization capacity in LTRs. Therefore, our findings suggest a benefit of repetitive vaccinations, especially concerning the humoral immune response, in this patient group.

In contrast to recent studies,[13,14] we only observed a small booster effect on the spike-specific CD4+ and CD8+ repertoire or the frequency of spike-specific CD8+ T cells after a third or fourth mRNA vaccine dose. This might be due to diverging timing of sampling between the different studies: Indeed, the data from Davidov *et al.*[13] and Harberts *et al.*,[14] demonstrating increased T-cell-mediated IFNγ production after booster vaccination, were collected within the peak effector phase (21-28 days and 12-21 days after booster vaccination, respectively). Our study, however, focused on the spike-specific T-cell epitope repertoire and spike-specific CD8+ T-cell memory pool within a more resting memory phase after two, three and four mRNA vaccine doses in LTRs. In HCs, this long-term spike-specific CD8+ T-cell memory pool remained conserved upon repeated vaccination, while a transient activation and expansion was elicited shortly after booster vaccination.[10] In addition, the spike-specific CD8+ and CD4+ T-cell repertoire in HCs was stable within 6 months after mRNA vaccination and remained unaffected throughout multiple vaccinations.[23] Our current data suggest that mRNA vaccination may induce similar kinetics in LTRs, with transient activation after booster vaccination and the formation of a stable long-term spike-specific T-cell memory. Interestingly, one LTR developed a spike-specific CD8+ T-cell response

above the detection threshold only after a fourth vaccine dose, arguing for a possible individual booster benefit in some LTRs.

Notably, the findings of our study are limited since, due to the complexity of the applied methods and the availability of suitable samples, we were only able to analyze a small number of patients, especially compared to studies with a more clinical focus. This not only impedes conclusions regarding potential risk factors (for example), but also limited our analyses regarding the frequency and phenotype of vaccine-induced CD8+ T cells to subsets directed against two different epitopes within the spike protein. However, considering the immunodominance of these epitopes,[8] it is very likely that our experiments are still conclusive.

In sum, we demonstrate that COVID-19 mRNA vaccination induces an overall robust humoral and cellular memory response in LTRs. Compared to HCs, development of high antibody titers requires a third vaccine dose in most LTRs, while spike-specific CD8+ T cells with robust recall capacity plateau after the second vaccine dose, albeit with a reduced frequency and epitope repertoire compared to HCs. This overall attenuated vaccine response is linked to a reduced T_{FH} cell frequency in LTRs. These results have important clinical implications: i) SARS-CoV-2 mRNA vaccination is a valuable preventive tool for the vulnerable cohort of LTRs, as it induces a robust memory immune response, ii) a third vaccine dose is of clear benefit for the majority of LTRs, and iii) additional booster doses may be of benefit for individual patients who have not adequately responded to the first three doses and may also be required depending on the evolution of viral VOC. The variance of vaccine response between LTRs also argues for the establishment of standardized and widely available assays to assess the cellular vaccine response in individuals with compromised immunity.

Affiliations

[1]Department of Medicine II (Gastroenterology, Hepatology, Endocrinology and Infectious Diseases), Freiburg University Medical Center, Faculty of Medicine, University of Freiburg, Freiburg, Germany; [2]IMM-PACT, Faculty of Medicine, University of Freiburg, Freiburg, Germany; [3]Faculty of Biology, University of Freiburg, Freiburg, Germany; [4]Institute for Immunodeficiency, Center for Chronic Immunodeficiency (CCI), University Medical Center, Faculty of Medicine, University of Freiburg, 79106 Freiburg, Germany; [5]Center for Pediatrics and Adolescent Medicine, University Medical Center, 79106 Freiburg, Germany; [6]Institute for Transfusion Medicine and Gene Therapy, Freiburg University Medical Center, Faculty of Medicine, University of Freiburg, Freiburg, Germany; [7]Institute of Virology, Faculty of Medicine, University Hospital Cologne, University of Cologne, Cologne, Germany; [8]Center for Molecular Medicine Cologne, University of Cologne, Cologne, Germany; [9]German Center for Infection Research, Partner Site Bonn-Cologne, Cologne, Germany; [10]Institute of Virology, Freiburg University Medical Center, Faculty of Medicine, University of Freiburg, Freiburg, Germany; [11]Signalling Research Centres BIOSS and CIBSS, University of Freiburg, Freiburg, Germany.

Abbreviations

AIM, activation-induced marker; HCs, healthy controls; LTRs, liver transplant recipients; OLPs, overlapping peptides; PBMCs, peripheral blood mononuclear cell; TFH, follicular T helper; TH, helper T; VOC, variants of concern.

Financial support

This study was supported by grants from the Deutsche Forschungsgemeinschaft (DFG, German Research Foundation; 272983813 to B.B., T.B., R.T., M.H. and C.N.H., and 256073931 to B.B., R.T., M.H. and C.N.H.; 413517907 to H.L. and J.L.M). This work was also supported by the project "Virological and immunological determinants of COVID-19 pathogenesis – lessons to get prepared for future pandemics (KA1-Co-02 "COVIPA")", a grant from the Helmholtz Association's Initiative and Networking Fund (to R.T. and M.H.). H.L. and J.L.M. are also supported by the IMM-PACT-Programme for Clinician Scientists, Department of Medicine II, Medical Center – University of Freiburg and Faculty of Medicine, University of Freiburg, funded by the Deutsche Forschungsgemeinschaft (DFG, German Research Foundation, 413517907). M.H. is also supported by the Margarete von Wrangell fellowship (State of Baden-Wuerttemberg). R.E. is supported by the Berta-Ottenstein-Programme for Advanced Clinician Scientists, Faculty of Medicine, University of Freiburg. T.B. is also supported by an Excellence Fellowship from the Else Kröner-Fresenius-Foundation. D.B.R. and A.G. are supported by the MOTI-VATE Programme, Faculty of Medicine, University of Freiburg. The funding bodies had no role in the decision to write or submit the manuscript.

Conflict of interest

The authors have nothing to declare.

Please refer to the accompanying ICMJE disclosure forms for further details.

Authors' contributions

H.L., D.B.R., J.L.M., M.R., M.E., E.S.A., K.W., A.G., V.K. planned, performed, and analyzed experiments. D.B., V.O., S., F.E., F.K., M.P., D.H., B.B., T.B. and R.E. collected clinical data and gave important intellectual input. R.T., M.H. and C.N.H. designed the study and contributed to experimental design and planning. H.L., D.B.R., J.L.M., R.T., M.H. and C.N.H. interpreted data and wrote the manuscript. All authors read and approved the final version of the manuscript.

Data availability statement

No data is deposited on public databases. All requests for raw and analyzed data and materials will be reviewed by the corresponding authors to verify if the request is subject to any confidentiality obligations. Patient-related data not included in the paper were generated as part of clinical examination and may be subject to patient confidentiality. Any data and materials that can be shared will be released via a material transfer agreement.

Acknowledgments

We thank all patients and healthy donors for participating in the current study.

Supplementary data

Supplementary data to this article can be found online at https://doi.org/10.1016/j.jhep.2023.02.007.

References

Author names in bold designate co-first authorship.

[1] Dumortier J, Duvoux C, Roux O, Altieri M, Barraud H, Besch C, et al. COVID-19 in liver transplant recipients: the French SOT COVID registry. Clin Res Hepatol Gastroenterol 2021;45:101639.

[2] **Guarino M**, **Cossiga V**, Loperto I, Esposito I, Ortolani R, Fiorentino A, et al. COVID-19 in liver transplant recipients: incidence, hospitalization and outcome in an Italian prospective double-centre study. Sci Rep 2022;12:4831.

[3] Cornberg M, Buti M, Eberhardt CS, Grossi PA, Shouval D. EASL position paper on the use of COVID-19 vaccines in patients with chronic liver diseases, hepatobiliary cancer and liver transplant recipients. J Hepatol 2021;74:944–951.

[4] Caballero-Marcos A, Salcedo M, Alonso-Fernandez R, Rodriguez-Peralvarez M, Olmedo M, Graus Morales J, et al. Changes in humoral immune response after SARS-CoV-2 infection in liver transplant recipients compared to immunocompetent patients. Am J Transpl 2021;21:2876–2884.

[5] D'Offizi G, Agrati C, Visco-Comandini U, Castilletti C, Puro V, Piccolo P, et al. Coordinated cellular and humoral immune responses after two-dose SARS-CoV2 mRNA vaccination in liver transplant recipients. Liver Int 2022;42:180–186.

[6] Guarino M, Cossiga V, Esposito I, Furno A, Morisco F. Effectiveness of SARS-CoV-2 vaccination in liver transplanted patients: the debate is open. J Hepatol 2022;76:237–239.

[7] Kalimuddin S, Tham CYL, Qui M, de Alwis R, Sim JXY, Lim JME, et al. Early T cell and binding antibody responses are associated with COVID-19 RNA vaccine efficacy onset. Med (N Y) 2021;2:682–688 e684.

[8] **Oberhardt V**, **Luxenburger H**, **Kemming J**, **Schulien I**, Ciminski K, Giese S, et al. Rapid and stable mobilization of CD8+ T cells by SARS-CoV-2 mRNA vaccine. Nature 2021;597:268–273.
[9] Rabinowich L, Grupper A, Baruch R, Ben-Yehoyada M, Halperin T, Turner D, et al. Low immunogenicity to SARS-CoV-2 vaccination among liver transplant recipients. J Hepatol 2021;75:435–438.
[10] **Reinscheid M**, **Luxenburger H**, **Karl V**, **Graeser A**, **Giese S**, **Ciminski K**, et al. COVID-19 mRNA booster vaccine induces transient CD8+ T effector cell responses while conserving the memory pool for subsequent reactivation. Nat Commun 2022;13:4631.
[11] Ruether DF, Schaub GM, Duengelhoef PM, Haag F, Brehm TT, Fathi A, et al. SARS-CoV2-specific humoral and T-cell immune response after second vaccination in liver cirrhosis and transplant patients. Clin Gastroenterol Hepatol 2022;20:162–172 e169.
[12] Toniutto P, Falleti E, Cmet S, Cussigh A, Veneto L, Bitetto D, et al. Past COVID-19 and immunosuppressive regimens affect the long-term response to anti-SARS-CoV-2 vaccination in liver transplant recipients. J Hepatol 2022;77:152–162.
[13] Davidov Y, Indenbaum V, Tsaraf K, Cohen-Ezra O, Likhter M, Ben Yakov G, et al. A third dose of the BNT162b2 mRNA vaccine significantly improves immune responses among liver transplant recipients. J Hepatol 2022;77:702–709.
[14] Harberts A, Schaub GM, Ruether DF, Duengelhoef PM, Brehm TT, Karsten H, et al. Humoral and cellular immune response after third and fourth SARS-CoV-2 mRNA vaccination in liver transplant recipients. Clin Gastroenterol Hepatol 2022;20:2558–2566.
[15] Toniutto P, Cussigh A, Cmet S, Bitetto D, Fornasiere E, Fumolo E, et al. Immunogenicity and safety of a third dose of anti-SARS-CoV-2 BNT16b2 vaccine in liver transplant recipients. Liver Int 2023;43:452–461.
[16] Nelson RW, Chen Y, Venezia OL, Majerus RM, Shin DS, Collection MC-, et al. SARS-CoV-2 epitope-specific CD4+ memory T cell responses across COVID-19 disease severity and antibody durability. Sci Immunol 2022;7:eabl9464.
[17] Wieland D, Kemming J, Schuch A, Emmerich F, Knolle P, Neumann-Haefelin C, et al. TCF1+ hepatitis C virus-specific CD8+ T cells are maintained after cessation of chronic antigen stimulation. Nat Commun 2017;8:15050.
[18] Sahin U, Muik A, Vogler I, Derhovanessian E, Kranz LM, Vormehr M, et al. BNT162b2 vaccine induces neutralizing antibodies and poly-specific T cells in humans. Nature 2021;595:572–577.
[19] Painter MM, Mathew D, Goel RR, Apostolidis SA, Pattekar A, Kuthuru O, et al. Rapid induction of antigen-specific CD4+ T cells is associated with coordinated humoral and cellular immunity to SARS-CoV-2 mRNA vaccination. Immunity 2021;54:2133–2142 e2133.
[20] Crotty S. T follicular helper cell biology: a decade of discovery and diseases. Immunity 2019;50:1132–1148.
[21] Cui C, Wang J, Fagerberg E, Chen PM, Connolly KA, Damo M, et al. Neoantigen-driven B cell and CD4 T follicular helper cell collaboration promotes anti-tumor CD8 T cell responses. Cell 2021;184:6101–6118 e6113.
[22] Zander R, Kasmani MY, Chen Y, Topchyan P, Shen J, Zheng S, et al. Tfh-cell-derived interleukin 21 sustains effector CD8+ T cell responses during chronic viral infection. Immunity 2022;55:475–493 e475.
[23] **Lang-Meli J**, **Luxenburger H**, **Wild K**, **Karl V**, **Oberhardt V**, Salimi Alizei E, et al. SARS-CoV-2-specific T-cell epitope repertoire in convalescent and mRNA-vaccinated individuals. Nat Microbiol 2022;7:675–679.

Journal of Hepatology, Volume ■

Supplemental information

Boosting compromised SARS-CoV-2-specific immunity with mRNA vaccination in liver transplant recipients

Hendrik Luxenburger, David B. Reeg, Julia Lang-Meli, Matthias Reinscheid, Miriam Eisner, Dominik Bettinger, Valerie Oberhardt, Elahe "Salimi Alizei", Katharina Wild, Anne Graeser, Vivien Karl, Sagar, Florian Emmerich, Florian Klein, Marcus Panning, Daniela Huzly, Bertram Bengsch, Tobias Boettler, Roland Elling, Robert Thimme, Maike Hofmann, and Christoph Neumann-Haefelin

Boosting compromised SARS-CoV-2-specific immunity with mRNA vaccination in liver transplant recipients

Hendrik Luxenburger, David B. Reeg, Julia Lang-Meli, Matthias Reinscheid, Miriam Eisner, Dominik Bettinger, Valerie Oberhardt, Elahe Salimi Alizei, Katharina Wild, Anne Graeser, Vivien Karl, Sagar, Florian Emmerich, Florian Klein, Marcus Panning, Daniela Huzly, Bertram Bengsch, Tobias Boettler, Roland Elling, Robert Thimme, Maike Hofmann, Christoph Neumann-Haefelin

Table of contents

Supplementary methods

PBMC isolation

Samples of venous blood were collected in EDTA-anticoagulated tubes. PBMCs were isolated with lymphocyte separation medium by density gradient centrifugation (Pancoll separation medium, PAN Biotech GmbH). PBMCs were stored at −80 °C. Frozen PBMCs were thawed in complete medium (RPMI 1640 supplemented with 10 % fetal calf serum, 1 % penicillin/streptomycin and 1.5 % HEPES buffer 1 M (all additives from Thermo Scientific) containing 50 U ml^{-1} benzonase (Sigma).

In vitro expansion and intracellular IFNγ staining with overlapping peptides

We tested a total of 182 overlapping peptides (OLPs) spanning the entire SARS-CoV-2 spike protein sequence (Gene Bank Accession code MN908947.3), synthesized as 18-mers overlapping by 11 amino acids with a free amine NH_2 terminus and a free acid COOH terminus with standard Fmoc chemistry showing a purity of > 70% (Genaxxon Bioscience). To perform the *in vitro* expansion with OLPs, we stimulated 20 % of the PBMCs with a pool of all 182 SARS-CoV-2 spike OLPs (10 µg ml^{-1}) for 1 h at 37 °C. Next, the cells were washed and co-cultured with the remaining PBMCs in RPMI medium supplemented with recombinant IL-2 (20 U ml^{-1}). On day 10, we performed intracellular IFNγ staining with pooled OLPs. Cells were re-stimulated with 45 OLP pools (50 µM) containing four peptides each (dimethylsulfoxid (DMSO) as negative control and phorbol 12-myristate 13-acetate (PMA) as well as ionomycin (50 ng ml^{-1} and 1 µg ml^{-1}) as positive control) in the presence of both brefeldin A (GolgiPlug, 0.65 µl ml^{-1}) and IL-2 (0.05 U ml^{-1}). Cells were stained for surface markers (CD8, CD4), viability (Viaprobe) and intracellular markers (IFNγ) after 5 h of incubation at 37 °C. On day 12, the single overlapping peptides of all positive pools were tested by intracellular cytokine staining. The viral amino acid sequences of positive individual OLPs were then screened for previously described minimal epitopes or the best HLA-matched predicted candidate using the Immune Epitope Database website (www.iedb.org) combined with two prediction algorithms ANN 4.0 and NetMHCpan EL 4.123 for 8-mer, 9-mer and 10-mer peptides with half-maximal inhibitory concentration (IC_{50}) of < 500 nM.

Magnetic bead-based enrichment of spike-specific CD8+ T cells

Enrichment of spike-specific CD8+ T cells was performed as described previously [1]. Briefly, 1 × 10^7–2 × 10^7 PBMCs were labelled with APC-coupled peptide-loaded HLA class I tetramers for half an hour. Next, the enrichment was performed using anti-APC beads with MACS technology (Miltenyi Biotec) according to the manufacturer's instructions. Subsequently, analysis of the enriched spike-specific CD8+ T cells was conducted by multiparametric flow cytometry and frequencies of spike-specific CD8+ T cells were calculated as described before [1]. Importantly, only samples including ≥ 5 spike-specific CD8 T cells were used for further subset gating and phenotypic analyses (detection limit of 5 × 10^{-6}).

SARS-CoV-2 pseudovirus neutralization assay

Pseudovirus neutralization assays against SARS-CoV-2 wild-type (Wuhan-Hu-1) and the Omicron variants BA.4/5 were performed on a selection of 47 samples as previously described [2-4]:

Cell lines: HEK293T cells and 293T-ACE2 cells

HEK293T cells and HEK293T-ACE2 cells [5] were grown in DMEM (Gibco) supplemented with 10 % FCS, 0,5 % Ciprofloxacin, 1 mM L-Glutamine and 1 mM Sodium pyruvate. Cells were maintained on tissue culture treated dishes in a T75 flask at 37 °C in a 5 % CO_2 humidified incubator.

Generation of spike pseudotyped lentiviral particles

For lentivirus production, adherent HEK 293T cells in T75 flasks were transfected with single plasmids encoding a fluorescent reporter protein (pHAGE-Luc-IRES-ZsGreen), a set of lentiviral proteins necessary for virion formation (pHDM-Hgpm, pHDM-Tat, pHDM-Rev) and the variant-specific spike protein (SARS-CoV-2 strain Wuhan-Hu-1 and Omicron VOC BA.4/5). For transfection, we used FuGENE 6 transfection reagent (Promega) according to manufacturer instructions. After 48 and 72 hours of incubation, we harvested the virus supernatant of the cell culture. Virus supernatants were centrifuged (400 g, 10 °C for 5 min), then filtered (0.45 µm filter) and stored in 1 ml aliquots at -80 °C until use.

Each viral batch was titrated by infection of 293T-ACE2. After incubation for 48 hours at 37 °C and 5 % CO2, the infectious titers of pseudovirus supernatants were assessed by adding luciferin/lysis buffer (10 mM $MgCl_2$, 0.3 mM ATP, 0.5 mM coenzyme A, 17 mM IGEPAL CA-630 (all Sigma-Aldrich), and 1 mM D-Luciferin (GoldBio) in Tris-HCL). Relative light units (RLUs) were measured with a microplate reader (TECAN SPARK).

SARS-CoV-2 pseudovirus neutralization assay

To quantify the SARS-CoV-2 neutralizing activity of serum samples, serial dilutions of serum (heat-inactivated at 56 °C for 30 minutes) were incubated with pseudovirus supernatants at 37 °C for 1 hour. 293T-ACE2 cells were added after the incubation period. Firefly luciferase activity was measured after 48 hours of incubation. The 50 % inhibitory dose (ID50) was defined as the serum dilution that resulted in a 50 % RLU reduction compared with the RLU signal from pseudovirus-infected cells without human serum (minus background luminescence). The serum samples were measured in technical duplicates and the average ID50 values are reported. ID50 values were determined in Prism 9 by plotting a dose-response curve.

References for Supplementary Methods

Author names in bold designate co-first authorship.

[1] Alanio C, Lemaitre F, Law HK, Hasan M, Albert ML. Enumeration of human antigen-specific naive CD8+ T cells reveals conserved precursor frequencies. Blood 2010;115:3718-3725.
[2] Gruell H, Vanshylla K, Tober-Lau P, Hillus D, Sander LE, Kurth F, et al. Neutralisation sensitivity of the SARS-CoV-2 omicron BA.2.75 sublineage. Lancet Infect Dis 2022;22:1422-1423.
[3] **Habermann E, Gieselmann L**, Tober-Lau P, Klotsche J, Albach FN, Ten Hagen A, et al. Pausing methotrexate prevents impairment of Omicron BA.1 and BA.2 neutralisation after COVID-19 booster vaccination. RMD Open 2022;8.
[4] Vanshylla K, Di Cristanziano V, Kleipass F, Dewald F, Schommers P, Gieselmann L, et al. Kinetics and correlates of the neutralizing antibody response to SARS-CoV-2 infection in humans. Cell Host Microbe 2021;29:917-929 e914.
[5] Crawford KHD, Eguia R, Dingens AS, Loes AN, Malone KD, Wolf CR, et al. Protocol and Reagents for Pseudotyping Lentiviral Particles with SARS-CoV-2 Spike Protein for Neutralization Assays. Viruses 2020;12.

Supplementary figures

Figure S1

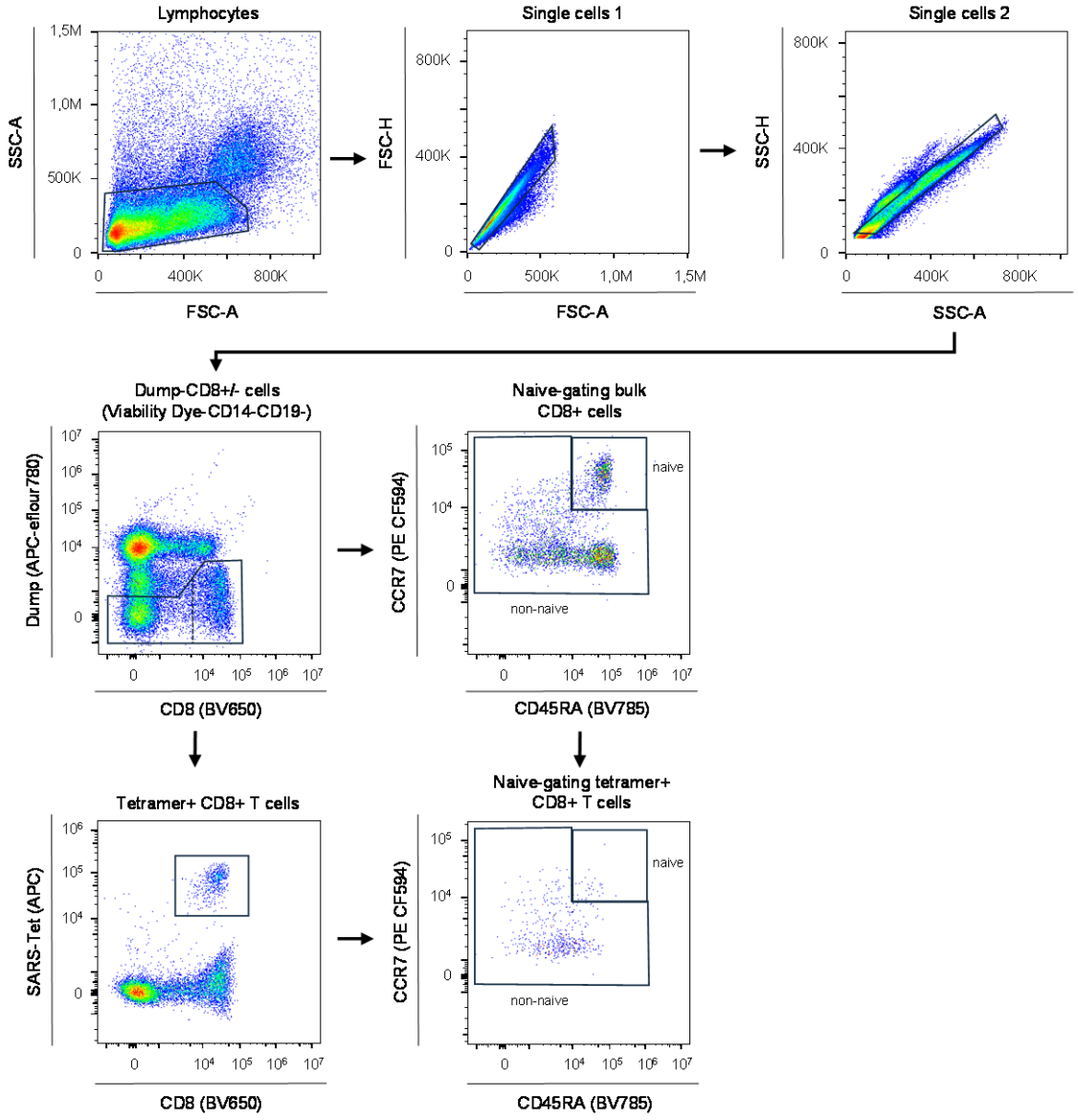

Fig. S1: Gating strategy peptide/MHC I tetramer enrichment.

Gating strategy of flow cytometry data to specify spike-reactive CD8+ T cells after peptide/MHC class I tetramer-enrichment

Figure S2

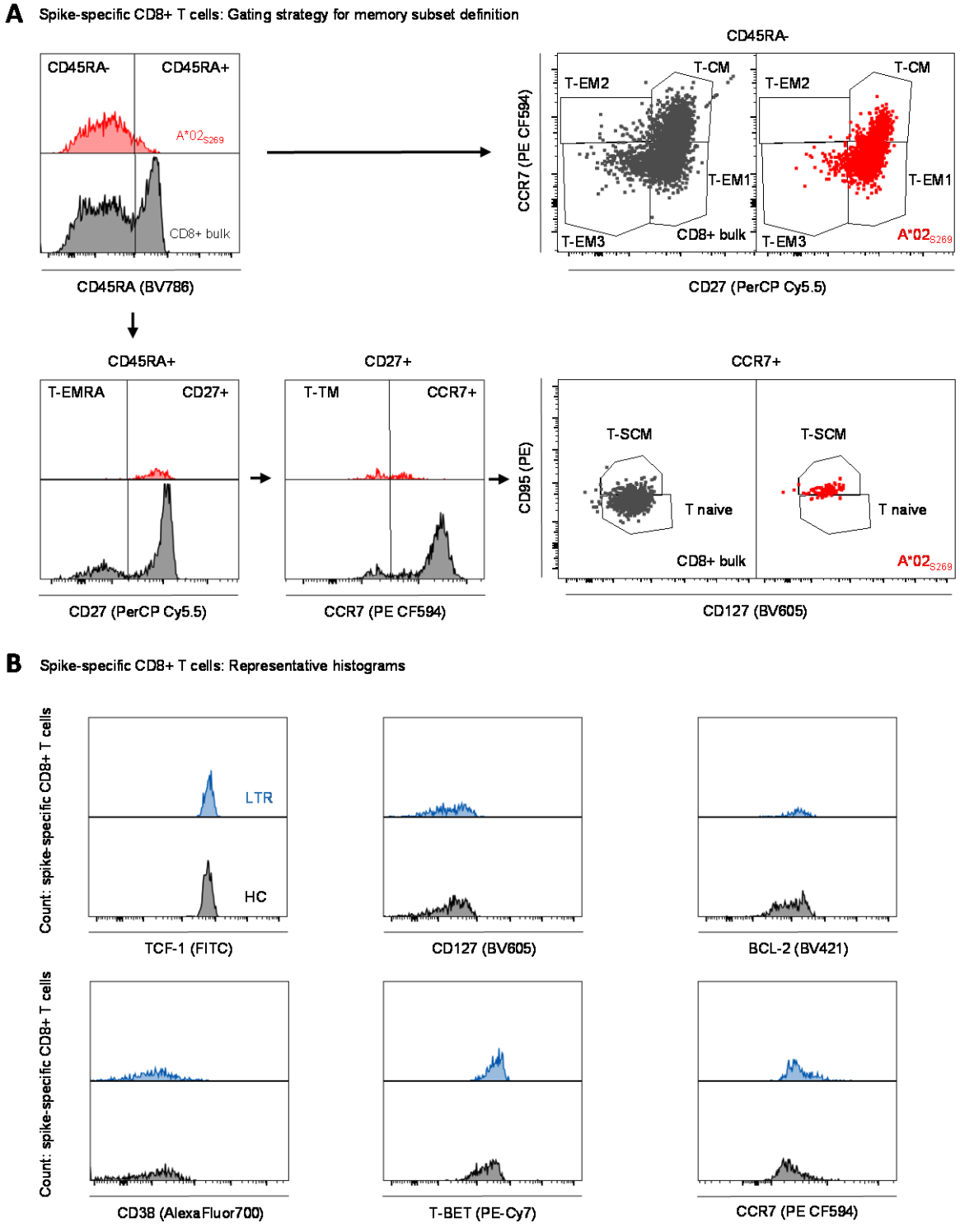

Fig. S2: Spike-specific CD8+ T memory cells.

(A) Gating strategy of flow cytometry data for memory subset specifications. This gating was applied to samples after *ex vivo* enrichment. **(B)** Representative histograms for indicated molecule expression on virus-specific CD8+ T cells after peptide/MHC I tetramer-enrichment in liver transplant recipients and healthy controls.

Figure S3

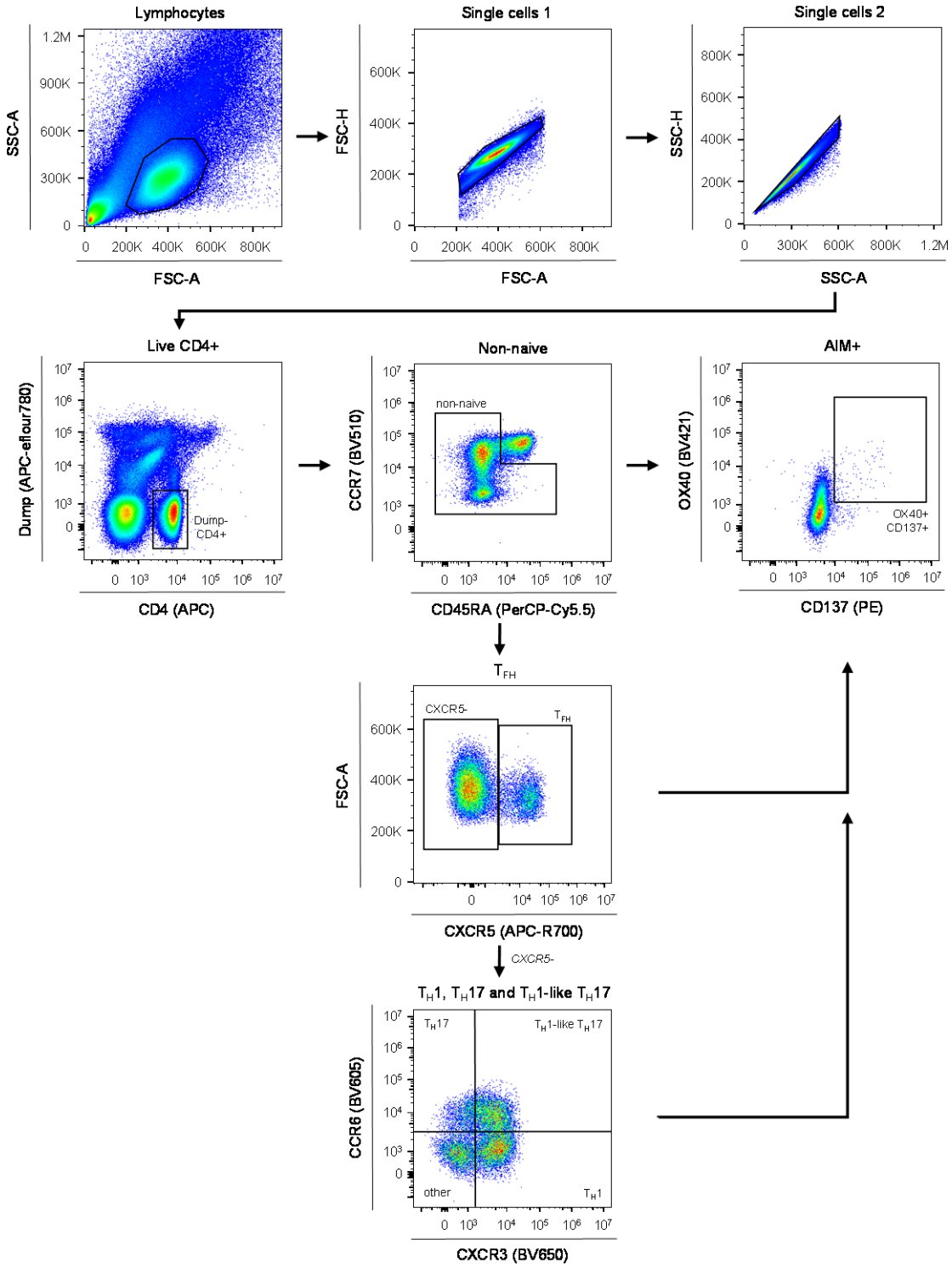

Fig. S3: Gating Strategy AIM-Assay.

Gating strategy to define AIM+ (CD137+ OX40+) non-naive CD4+ T cells and the respective CD4+ T cell subsets.

Figure S4

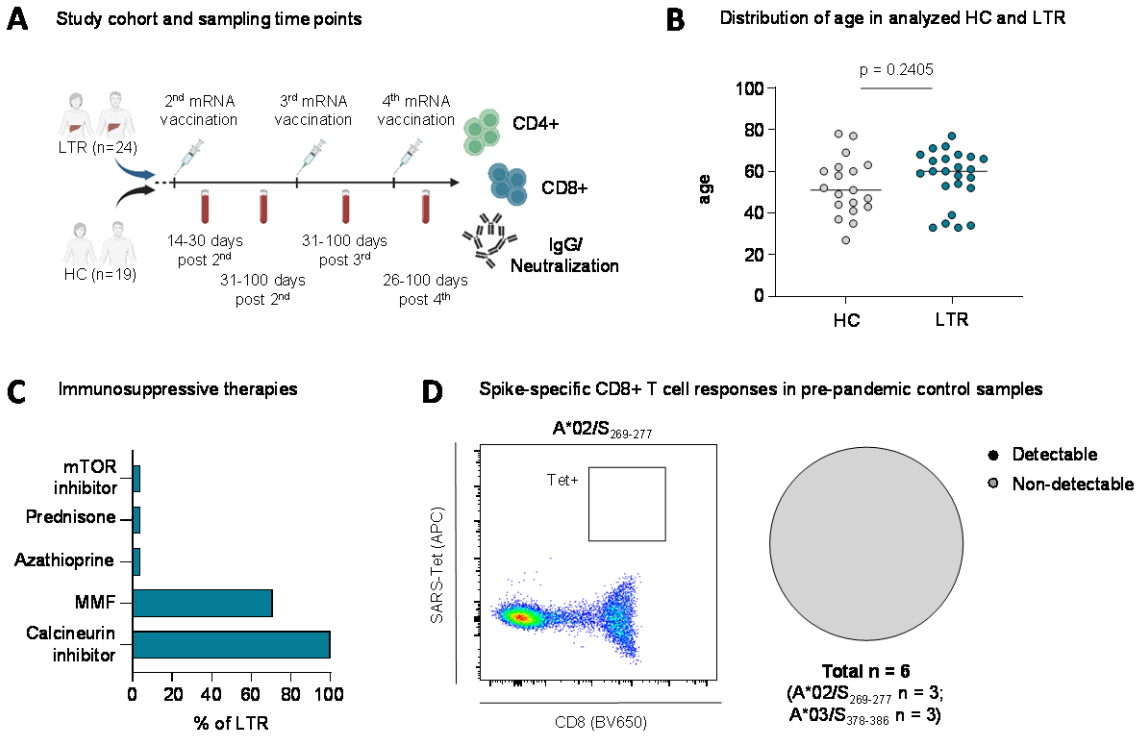

Fig. S4: Clinical parameters and spike-specific CD8+ T cell activation in LTR.

(A) Overview of study cohort and sampling time points. **(B)** Age of HC (n=19) and LTR (n=24) **(C)** Immunosuppressive therapy of LTR enrolled in this study (n=24). **(D)** Representative dot plot and percentage of pre-pandemic control samples with detectable/non-detectable response after tetramer-based enrichment. Statistics: Mann-Whitney test (B). HC: healthy control; LTR: liver transplant recipient; MMF: mycophenolate mofetil.

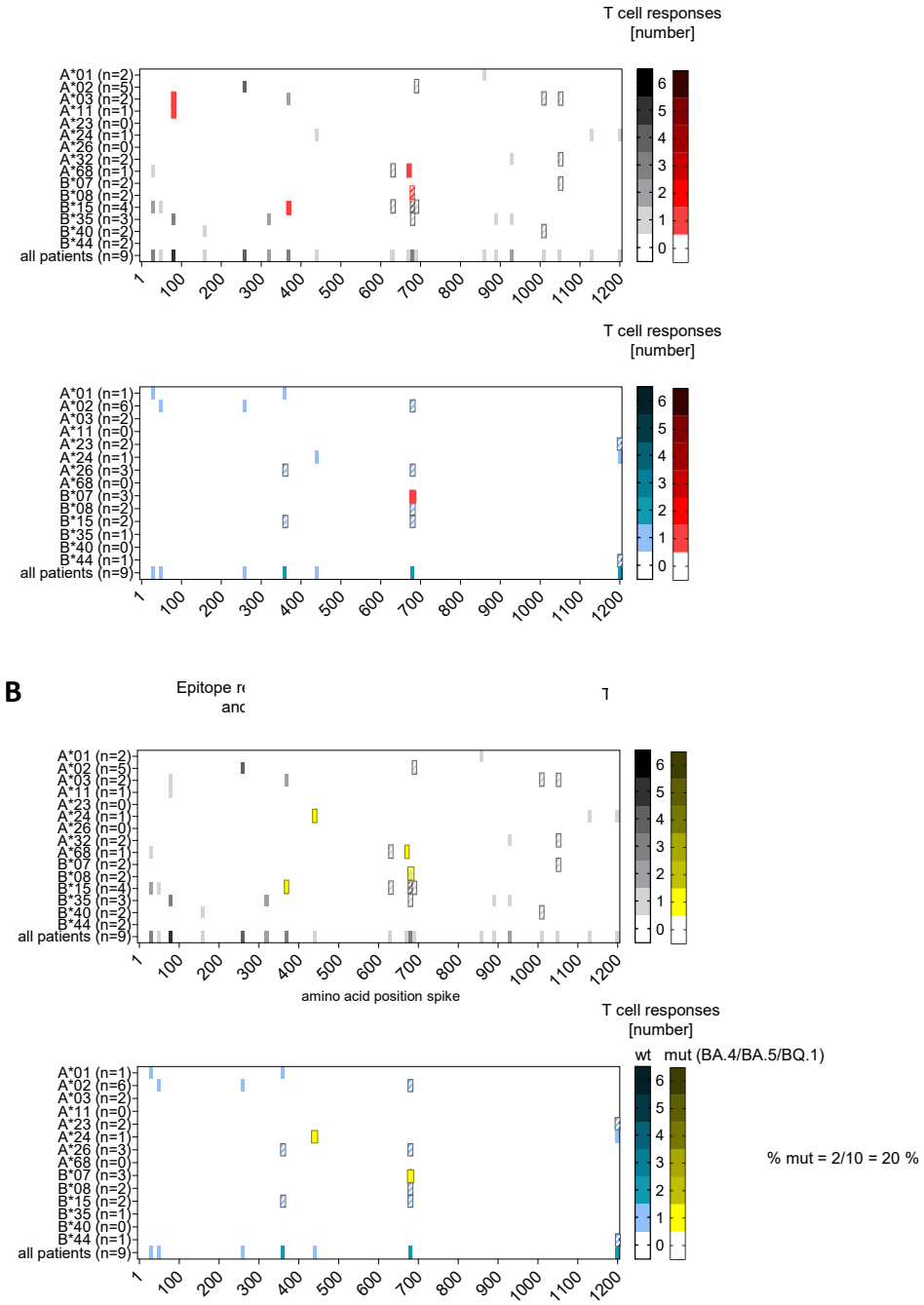

Fig. S5: CD8+ T cell responses targeting wild-type or variant spike-specific epitopes

Number and location of spike-specific CD8 + T cell responses to overlapping peptides (OLP) in HC and LTR after three vaccine doses. **(A)** Epitopes with amino acid sequence variations in Omicron BA.1 are marked in red. **(B)** Epitopes with amino acid sequence variations in Omicron BA.4/5 and BQ.1 are marked in yellow. Numbers of tested individuals (per HLA allotype and in total) and the percentage of total T cell responses targeting variant epitopes are indicated.

Figure S6

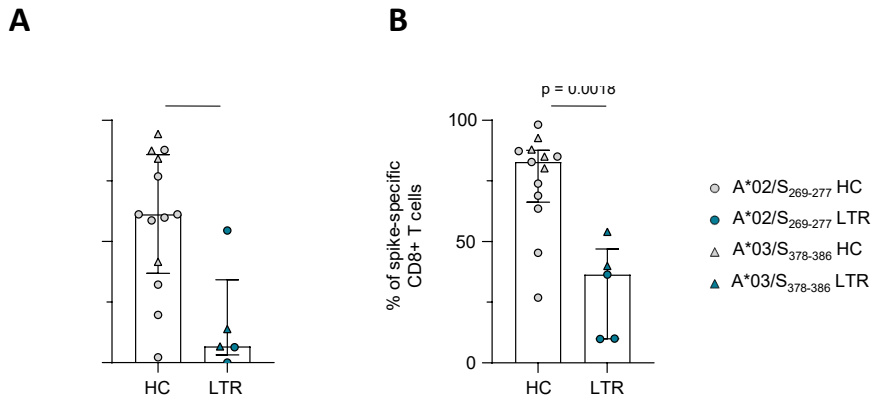

Fig. S6: Activation and effector differentiation of spike-specific CD8+ T cells after the 2nd vaccine dose.

(A) Percentage of spike-specific CD8+ T cells with T-BET^{hi} expression at 14-30 days post 2nd vaccine dose. **(B)** Percentage of CD38+ spike-specific CD8+ T cells at 14-30 days post 2nd vaccine dose. Statistics: Mann-Whitney test (A, B).

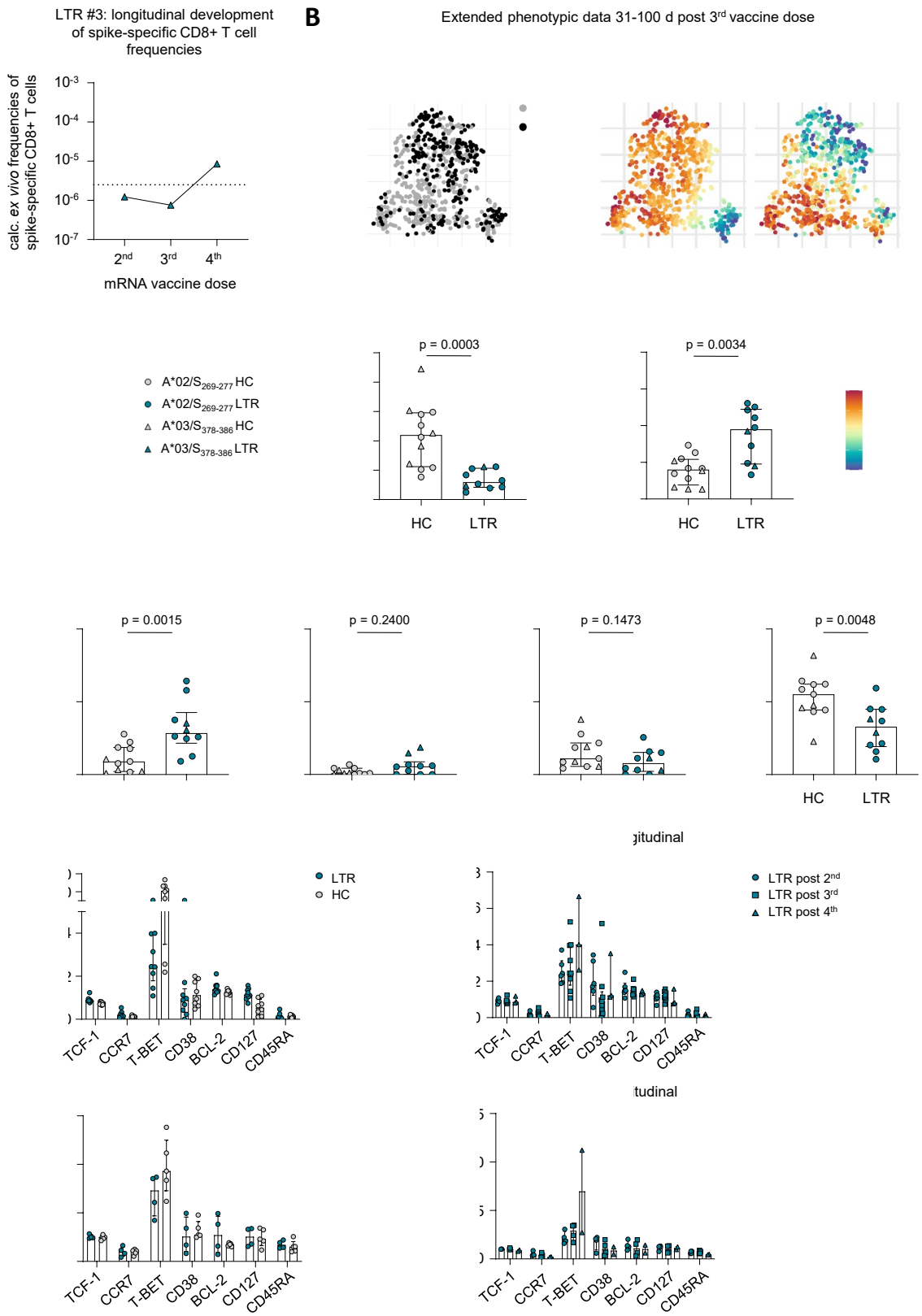
LTR #3: longitudinal development of spike-specific CD8+ T cell frequencies
calc. ex vivo frequencies of spike-specific CD8+ T cells
10-3
10-4
10-5
10-6
10-7
2nd
3rd
4th
mRNA vaccine dose
B
Extended phenotypic data 31-100 d post 3rd vaccine dose
A*02/S269-277 HC
A*02/S269-277 LTR
A*03/S378-386 HC
A*03/S378-386 LTR
p = 0.0003
p = 0.0034
HC
LTR
p = 0.0015
p = 0.2400
p = 0.1473
p = 0.0048
HC
LTR
gitudinal
LTR
HC
LTR post 2nd
LTR post 3rd
LTR post 4th
TCF-1
CCR7
T-BET
CD38
BCL-2
CD127
CD45RA
tudinal

Fig. S7: Marker expression and memory CD8+ T cell subset distribution in HC versus LTR.

(A) Calculated *ex vivo* frequencies of spike-specific CD8+ T cells for patient LTR#3 at 14-30 days after the 2nd, 31-100 days after the 3rd or 26-100 days after the 4th vaccine dose. **(B)** t-SNE representation or bar graphs of flow cytometry data comparing spike-specific CD8+ T cells with CD38, T-BET or CD127 expression derived from HC and LTR 31-100 days after the 3rd vaccine dose. **(C)** Spike-specific CD8+ T cells with central memory (T-CM; CD45RA-CCR7+CD27+), stem cell memory (T-SCM; CD45RA+CCR7+CD27+CD95+), transitional memory (T-TM; CD45RA+CCR7-CD27+) and effector memory (T-EM; CD45RA-CCR7-CD27+) phenotype in LTR versus HC at 31-100 days post 3rd vaccine dose (LTR n=10, HC n=11). **(D)** Individual fluorescence intensity (nMFI) of different markers within the subset of BCL-2^{hi} or T-SCM spike-specific CD8+ T cells in HC and LTR normalized to naïve CD8+ T cells; samples with ≥ 5 cells per subset are depicted. Statistics: Mann-Whitney test (B, C). HC: healthy control; LTR: liver transplant recipient.

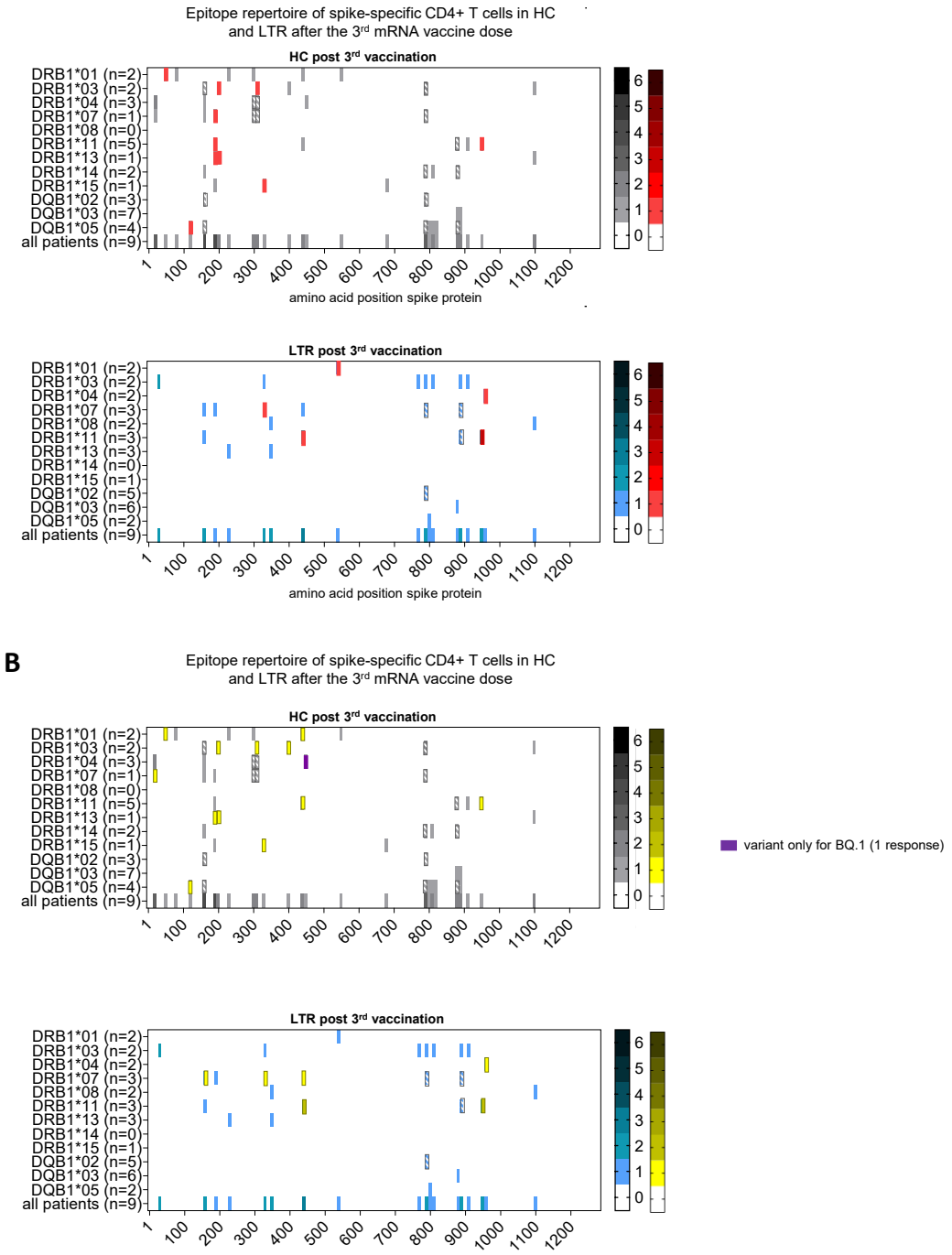

Fig. S8: CD4+ T cell responses targeting wild-type or variant spike-specific epitopes

Number and location of spike-specific CD4+ T cell responses to overlapping peptides (OLP) in HC and LTR after three vaccine doses. **(A)** Epitopes with amino acid sequence variations in Omicron BA.1 are marked in red. **(B)** Epitopes with amino acid sequence variations in Omicron BA.4/5 and BQ.1 are marked in yellow. Numbers of tested individuals (per HLA allotype and in total) and the percentage of total T cell responses targeting variant epitopes are indicated.

Figure S9

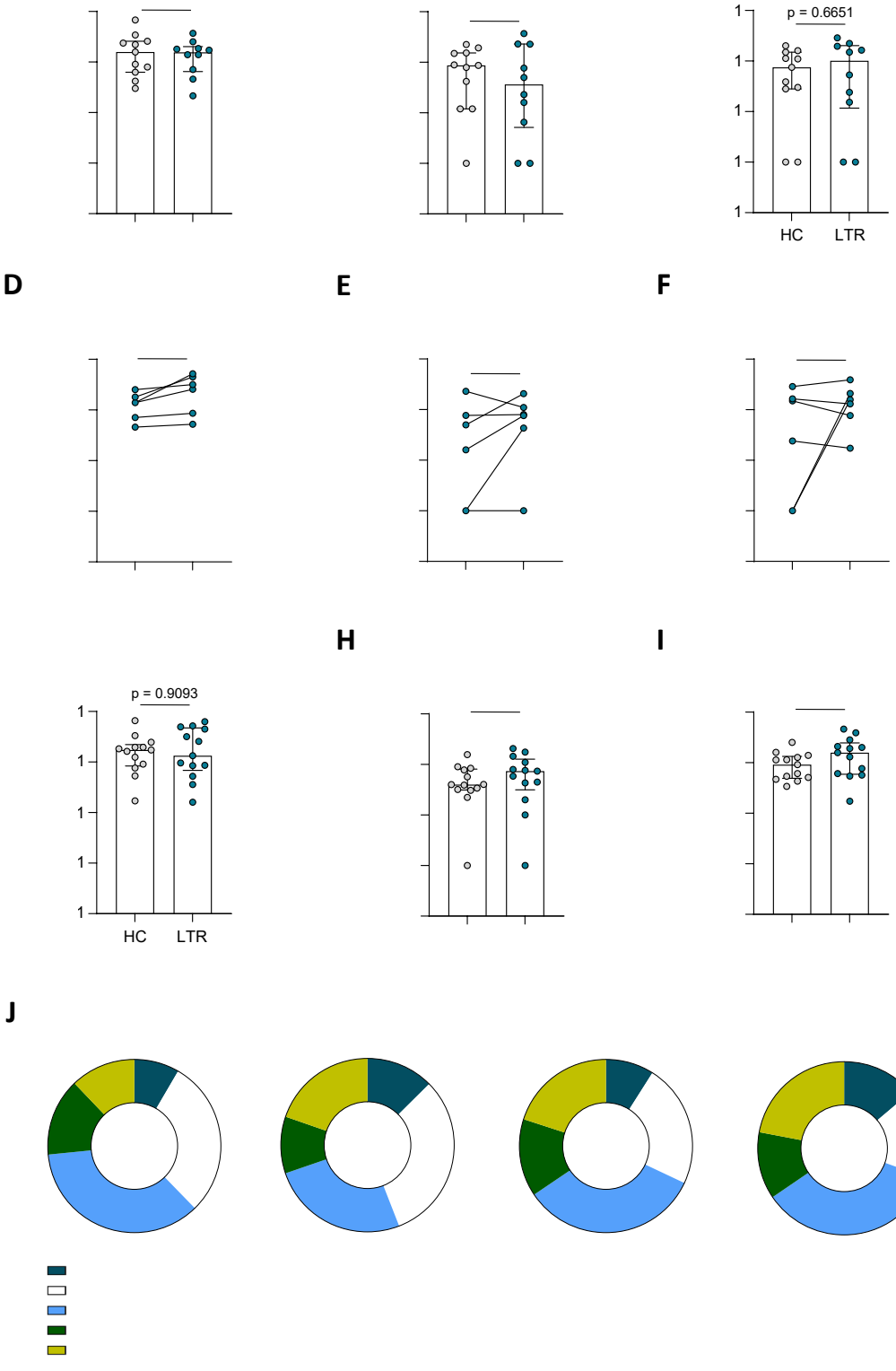

Fig. S9: Subset distribution of spike-specific CD4$^+$ T cells in HC and LTR.

(A-C) Frequencies of spike-specific T_H1 (A), T_H17 (B) and T_H1-like T_H17 (C) cells in HC (n=11) and LTR (n=10) after the 2nd vaccine dose. **(D-F)** Longitudinal development of the frequencies of spike-specific T_H1, T_H17 and T_H1-like T_H17 cells after the 2nd and 3rd vaccine dose in LTR (n=6). **(G-I)** Frequencies of spike-specific T_H1, T_H17 and T_H1-like T_H17 cells in HC (n=13) and LTR (n=13) after the 3rd vaccine dose. **(J)** Subset distribution of spike-specific CD4+ T cells in HC and LTR after the 2nd or 3rd vaccine dose. Statistics: Mann-Whitney test (A-C, G-I) and Wilcoxon matched-pairs signed rank test (D-F). HC: healthy control; LTR: liver transplant recipient.

Figure S10

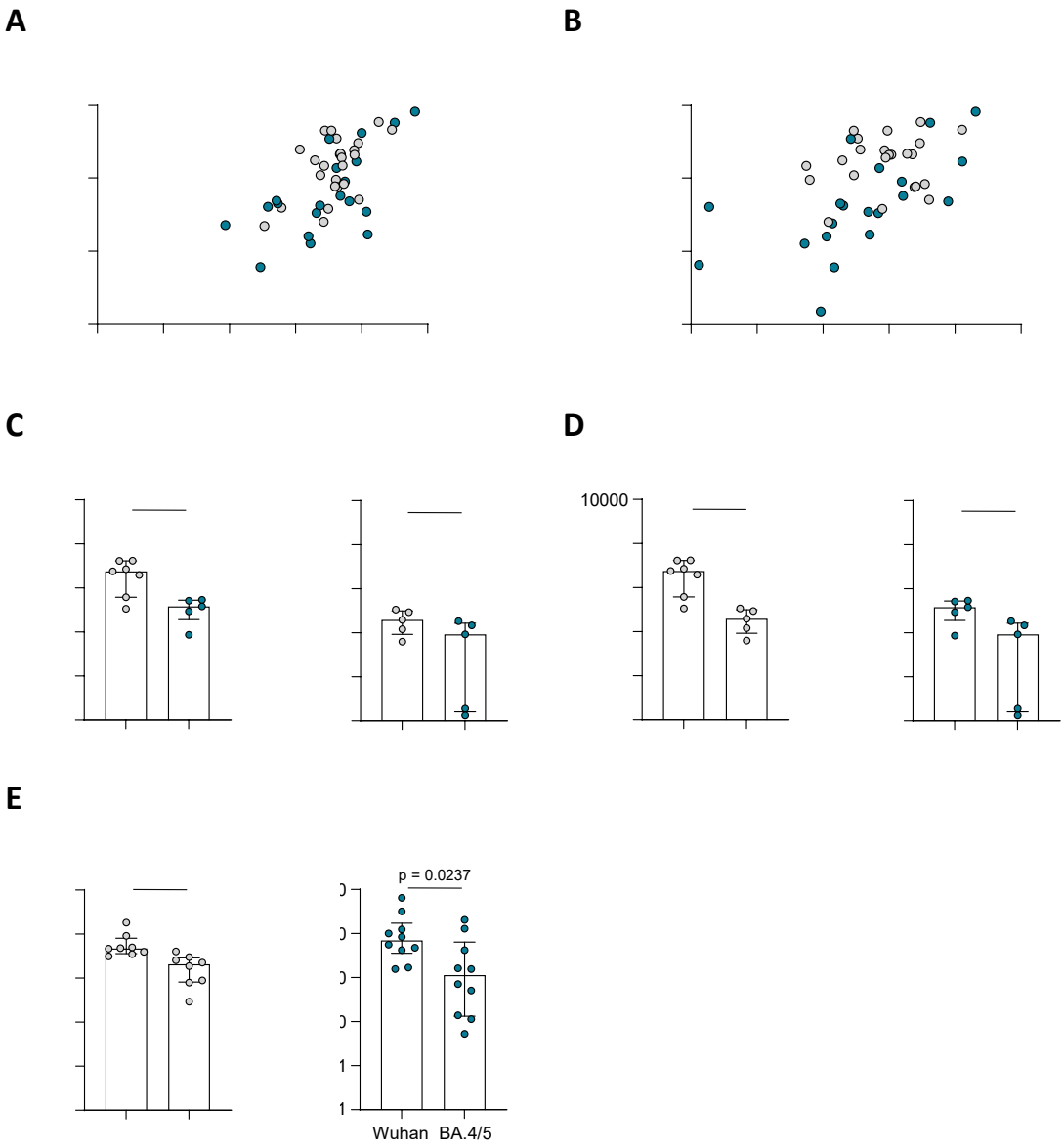

Fig. S10: Neutralizing capacity and spike-specific IgG in HC and LTR.

(A, B) Correlation between level of spike-specific IgG and neutralizing capacity against Wuhan (A) and Omicron BA.4/5 (B) variants. LTR and HC as well as all available vaccination time points were pooled for the correlation analysis. **(C, D)** Neutralizing capacity against SARS-CoV-2 Wuhan variant or Omicron BA.4/5 variants in HC (n=7 or 5, respectively) and LTR (n=5) after the 2nd vaccine dose. **(E)** Neutralizing capacity against SARS-CoV-2 Wuhan variant or Omicron BA.4/5 variant in HC (n=8) and LTR (n=10) after the 3rd vaccine dose. Statistics: Mann-Whitney test (C-E), Spearman correlation (A, B). HC: healthy control; LTR: liver transplant recipient

Table S1: Patient characteristics

Donor ID	Sex	Age	Years since transplantation	Etiology of liver disease	Immuno-suppression	HLA Type	1st vaccine dose	2nd vaccine dose	3rd vaccine dose	4th vaccine dose	OLP	Tested CD8+ T cell epitopes	AIM-Assay	Serum S-IgG1 assay
LTR 1	f	33	2	DILI	Tacrolimus, MMF	A*02:05, A*03:02, B*08:01, B*41:01	BNT162b2	BNT162b2	mRNA-1273	-	yes	-	yes	yes
LTR 2	f	60	9	other	Tacrolimus, MMF	A*02:01, A*24:02, B*07:02, B*15:17	BNT162b2	BNT162b2	BNT162b2	BNT162b2	yes	A*02/S269-277	no	yes
LTR 3	m	67	9	ALD	Ciclosporine, MMF	A*02:01, A*03:01, B*44:02, B*51:01	BNT162b2	BNT162b2	BNT162b2	BNT162b2	yes	A*03/S378-387	no	yes
LTR 4	m	58	4	ALD	Tacrolimus, MMF	A*02:01, A*26:01, B*13:02, B*39:01	BNT162b2	BNT162b2	BNT162b2	-	yes	A*02/S269-277	no	yes
LTR 5	m	66	25	ALD	Tacrolimus, MMF	A*03:01, A*29:02, B*07:02, B*27:05	BNT162b2	BNT162b2	BNT162b2	-	yes	A*03/S378-387	no	yes
LTR 6	m	68	7	viral hepatitis	Ciclosporine, MMF	A*02:02, A*23:01, B*41:01, B*44:03	BNT162b2	BNT162b2	BNT162b2	-	yes	-	no	yes
LTR 7	f	34	1	PSC	Ciclosporine, MMF	A*02:01, A*24:02, B*07:02, B*35:02	BNT162b2	BNT162b2	BNT162b2	-	yes	A*02/S269-277	yes	yes
LTR 8	m	57	1	NASH	Tacrolimus, MMF	A*02:01, A*30:01, B*07:02, B*13:02	BNT162b2	BNT162b2	BNT162b2	-	yes	A*02/S269-277	no	yes
LTR 9	m	61	23	other	Tacrolimus, MMF	A*01:01, A*02:01, B*08:01, B*27:05	BNT162b2	BNT162b2	BNT162b2	-	no	A*02/S269-277	yes	yes
LTR 10	m	39	2	NASH	Ciclosporine	A*03:01, A*11:01, B*07:02, B*35:03	BNT162b2	BNT162b2	BNT162b2	-	no	A*03/S378-387	no	yes
LTR 11	m	71	5	PSC	Tacrolimus, MMF	A*02:01, A*26:01, B*08:01, B*15:01	BNT162b2	BNT162b2	BNT162b2	BNT162b2	yes	A*02/S269-277	no	yes
LTR	m	33	5	PSC	Everolimus,	A*01:01, A*02:01,	BNT162b2	BNT162b2	mRNA-	-		A*02/S269-		

12					Tacrolimus, Prednison	B*07:02, B*51:01			1273		yes	277	yes	yes
LTR 13	f	52	28	other	Ciclosporine	A*03:01, B*35:03	BNT162b2	BNT162b2	mRNA-1273	-	no	A*03/S378-387	no	yes
LTR 14	f	60	14	PSC	Tacrolimus, Everolimus	A*01:01, A*03:01, B*08:01, B*40:01	BNT162b2	BNT162b2	BNT162b2	-	no	A*03/S378-387	no	yes
LTR 15	m	66	2	ALD	Tacrolimus, MMF	A*31:01, A*69:01, B*35:01, B*49:01	mRNA-1273	mRNA-1273	BNT162b2	BNT162b2	yes	-	yes	yes
LTR 16	m	62	8	PSC	Ciclosporin, MMF, Azathioprin	A*01:01, A*24:02, B*07:02, B*08:01	BNT162b2	BNT162b2	BNT162b2	-	no	A*01/S865-873	yes	yes
LTR 17	m	59	6	viral hepatitis	Ciclosporine, MMF	A*23:01, A*26:01, B*18:01, B*49:01	BNT162b2	BNT162b2	BNT162b2	-	no	-	yes	yes
LTR 18	f	77	9	viral hepatitis	Tacrolimus, MMF	A*32:01, B*35:01	BNT162b2	BNT162b2	BNT162b2	-	no	-	yes	yes
LTR 19	m	68	10	viral hepatitis	Tacrolimus, MMF	A*24:02, A*25:01, B*18:01, B*53:01	BNT162b2	BNT162b2	BNT162b2	-	no	-	yes	yes
LTR 20	m	65	4	NASH	Tacrolimus	A*02:01, A*68:01, B*27:05, B*51:01	BNT162b2	BNT162b2	BNT162b2	BNT162b2	no	A*02/S269-277	no	yes
LTR 21	m	72	13	NASH	Tacrolimus, MMF	A*02:01, A*68:01, B*44:02, B*44:03	BNT162b2	BNT162b2	BNT162b2	-	no	A*02/S269-277	yes	yes
LTR 22	m	53	21	SBC	Tacrolimus, MMF	A*02:01, B*41:01, B*51:01	BNT162b2	BNT162b2	BNT162b2	-	no	A*02/S269-277	yes	yes
LTR 23	m	54	1	PSC	Tacrolimus, MMF	A*02:01, B*08:01	BNT162b2	BNT162b2	-	-	no	A*02/S269-277	no	yes
LTR 24	m	35	8	other	Tacrolimus, MMF	A*01:01, A*02:01, B*13:02, B*40:01	BNT162b2	BNT162b2	BNT162b2	-	no	A*02/S269-277	no	yes
HC1	m	60	-	-	-	A*02:01, A*02:01, B*08:01, B*15:01	BNT162b2	BNT162b2	BNT162b2	BNT162b2	yes	A*02/S269-277	yes	yes
HC2	f	52	-	-	-	A*02:01, A*68:01, B*15:01, B*44:02	BNT162b2	BNT162b2	BNT162b2	-	yes	A*02/S269-277	yes	yes

HC3	m	47	-	-	-	A*02:01, A*24:02, B*27:05, B*51:01	BNT162b2	BNT162b2	BNT162b2	-	yes	A*02/S269-277	yes	yes
HC4	f	44	-	-	-	A*01:01, A*11:01, B*15:17, B*35:01	BNT162b2	BNT162b2	BNT162b2	mRNA-1273	yes	A*01/S865-873	yes	yes
HC5	m	43	-	-	-	A*03:01, A*32:01, B*07:02, B*40:02	BNT162b2	BNT162b2	mRNA-1273	-	yes	A*03/S378-387	no	yes
HC6	m	41	-	-	-	A*01:01, A*03:01, B*08:01, B*35:01	BNT162b2	BNT162b2	mRNA-1273	-	yes	A*03/S378-387	no	yes
HC7	f	35	-	-	-	A*01:01, A*03:01, B*07:02, B*57:01	BNT162b2	BNT162b2	BNT162b2	-	yes	A*03/S378-387	yes	yes
HC8	m	62	-	-	-	A*01:01, A*02:01, B*08:01, B*15:01	BNT162b2	BNT162b2	BNT162b2	-	yes	A*02/S269-277	no	yes
HC9	f	60	-	-	-	A*02:01, B*07:02, B*44:02	BNT162b2	BNT162b2	BNT162b2	-	yes	A*02/S269-277	yes	yes
HC10	m	69	-	-	-	A*02:01, B*13:02, B*15:01	BNT162b2	BNT162b2	mRNA-1273	-	yes	A*02/S269-277	yes	yes
HC11	m	77	-	-	-	A*31:01, A*32:01, B*35:01, B*40:02	BNT162b2	BNT162b2	BNT162b2	-	yes	-	yes	yes
HC12	f	78	-	-	-	A*02:01, A*03:01, B*07:02, B*18:01	BNT162b2	BNT162b2	BNT162b2	-	yes	A*03/S378-387	no	yes
HC13	m	37	-	-	-	A*02:01, A*68:01, B*15:01, B*51:01	BNT162b2	BNT162b2	BNT162b2	mRNA-1273	no	A*02/S269-277	yes	yes
HC14	f	63	-	-	-	A*02:01, A*03:01, B*27:05, B*37:01	BNT162b2	BNT162b2	BNT162b2	-	no	A*02/S269-277	yes	yes
HC15	f	49	-	-	-	A*03:01, A*69:01, B*35:08, B*51:01	BNT162b2	BNT162b2	BNT162b2	-	no	-	no	yes
HC16	f	51	-	-	-	A*03:01, B*07:02, B*27:05	BNT162b2	BNT162b2	-	-	no	A*03/S378-387	yes	yes
HC17	f	45	-	-	-	A*02:01, A*33:03,	BNT162b2	BNT162b2	-	-	no	-	yes	yes

						B*44:03, B*58:01								
HC18	f	27	-	-	-	A*02:01, A*02:02, B*41:01, B*57:01	BNT162b2	BNT162b2	BNT162b2	BNT162b2	no	A*02/S269-277	no	yes
HC19	m	58	-	-	-	A*01:01, A*03:01, B*08:01, B*35:01	BNT162b2	BNT162b2	BNT162b2	mRNA-1273	no	A*03/S378-387	no	yes

m: male; f: female; MMF: mycophenolate mofetil; S-IgG: spike-specific immunoglobulin G; DILI: Drug-induced liver injury; ALD: alcoholic liver disease; NASH: nonalcoholic steatohepatitis; PSC: primary sclerosing cholangitis; SBC: secondary biliary cholangitis; LTR: liver transplant recipient; HC: healthy control